Research Article

# On the energy budget of quarks and hadrons, their vastly underrated “strong charge,” and the profound impact of Coulomb repulsion on their ground states

**DImitris M. Christodoulou**[1], **Deosthenes Kazanas**[2]

1. Lowell Center for Space Science and Technology, University of Massachusetts at Lowell, United States; 2. Goddard Space Flight Center, Greenbelt, United States

**We meta-analyze particle data and properties for those hadrons with measured rest-masses. The results of our study are as follows: (1) the strong-force suppression of the repulsive Coulomb forces between quarks is sufficient to explain the differences between mass deficits in nucleons and pions (and only them), the ground states with the longest known mean lifetimes; (2) unlike mass deficits, the excitations in rest-masses of all particle groups are effectively quantized, but the rules are different in baryons and mesons; (3) the strong field is aware of the extra factor of $\vartheta_{\mathrm{e}} = 2$ in the charges $Q$ of the positively-charged quarks; (4) mass deficits combine contributions proportional to the mass of each valence quark; (5) the scaling factor of these contributions is the same for each quark in each group of particles, provided that the factor $\vartheta_{\mathrm{e}} = 2$ is taken into account; (6) besides hypercharge $Y$, the much lesser-known "strong charge" $Q' = Y - Q$ is very useful in SU(3) in describing properties of particles located along the right-leaning sides and diagonals of the weight diagrams; (7) strong decays in which $Q'$ is conserved are differentiated from weak decays, even for the same particle; (8) the energy diagrams of (anti)quark transitions indicate the origin of CP violation.**

**Corresponding authors:** DImitris M. Christodoulou, dimitris christodoulou@uml.edu; Deosthenes Kazanas, demos.kazanas@nasa.gov

 doi.org/10.32388/ZM7QNO 

# 1. Introduction

We have revisited the experimental results and the quantum properties relating to hadrons with measured rest-masses. Our data come from the extensive work of the Particle Data Group and from CODATA constants [1][2][3]. In this work, we focus on the mass deficits of particles and on the SU(3) quantum numbers that describe symmetries of the strong force. Our compilations of properties and derived quantum numbers are shown in Tables 1-3 for baryons with spin-parities $J^{\mathrm{P}} = (1/2)^{+}$ and $J^{\mathrm{P}} = (3/2)^{+}$, as well as for pseudo-scalar mesons with $J^{\mathrm{P}} = 0^{-}$ and vector mesons with $J^{\mathrm{P}} = 1^{-}$. Following standard convention, masses and mass deficits are listed in units of energy (MeV), and electromagnetic (EM) charges $Q$ are listed in units of the elementary charge.

In § 2, we analyze the mass deficits (MDs) of various particle groups, and we show that they can be described by the same scaling factors (binding factors $BF$ in Tables 1-3) of the valence quarks in each group. We also illustrate that it is the rest-masses $M$ of the various particles in a group (as opposed to MDs) that on average show hints of regularity and quantization at low energies. Detailed maps of the discrete jumps in rest-mass, without involving averaging, are deferred to Appendix A.

In § 3, we show that differences in the mass deficits (thus, also the observed differences in rest-energies) in nucleons and pions (listed under $MD$ in Tables 1 and 3) are almost entirely due to the strong force neutralizing the two repulsive Coulomb components between quarks with the same polarity. These repulsions develop only in charged particles ($Q \neq 0$). As would be expected, the same explanation is not sufficient for higher-energy particles (excited and resonant states).

In § 4, we introduce a combined quantum number, $Q' = Y - Q$, that represents the "strong piece" of the hypercharge $Y$. This "strong charge" describes the SU(3) symmetry of particles along the right-leaning sides and diagonals of the various weight diagrams (e.g., Figures 1-3); it is conserved only in strong interactions in which $Y$ is conserved, but it does not depend on $Q$; and it is the only quantum number (EM, weak, or strong) with a $(-1/3, 2/3)$ symmetry in each quark generation with increasing quark mass (Table 4).

In § 5, we classify the most common hadron decays into strong, EM, and weak categories based on a single quantum number, the strong charge $Q'$. This classification scheme is a new result, and it demonstrates the authority of this previously neglected (thus, vastly underrated, if at all known) quantum number, especially for particles that exhibit different types of decay in different channels.

In § 6, we discuss our results, and we raise some new questions about the nature of the known hadrons.

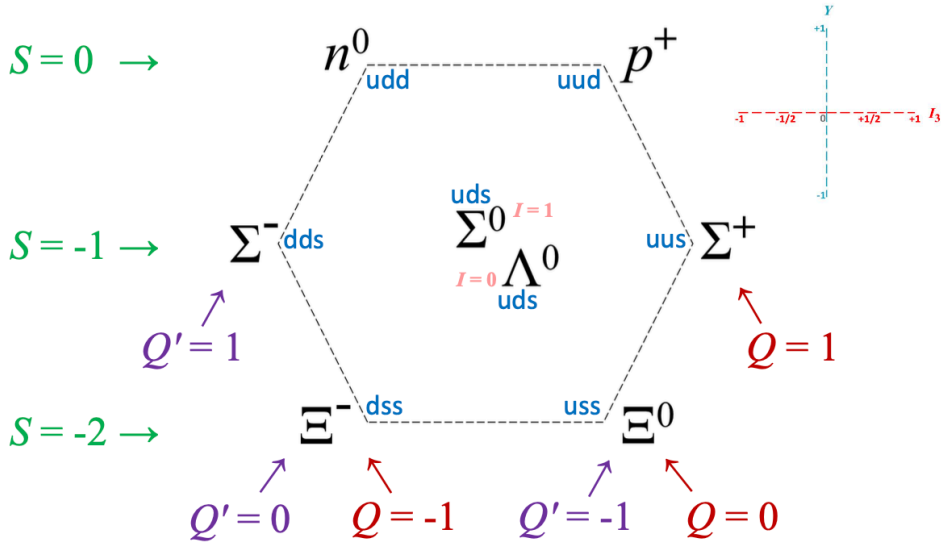


**Figure 1.** The weight diagram of the spin-parity $J^{\mathrm{P}} = (1/2)^{+}$ baryon octet.

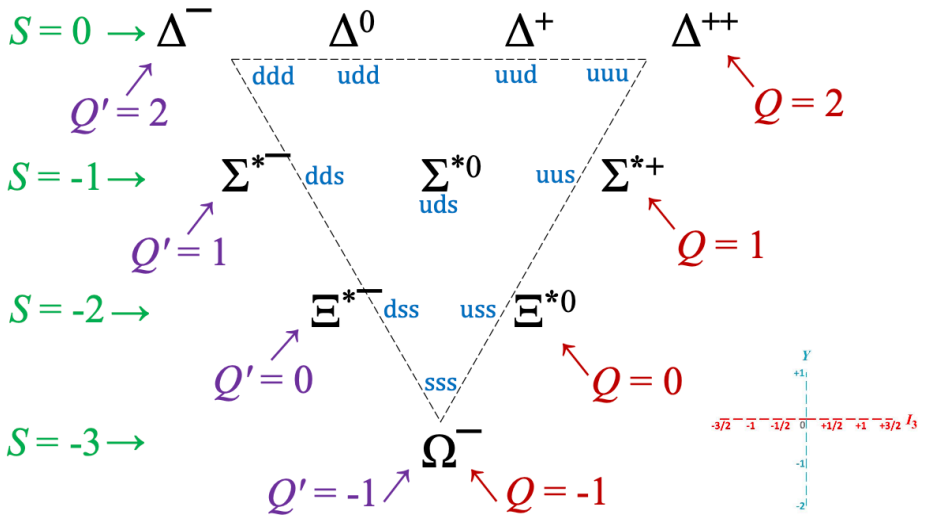


**Figure 2.** The weight diagram of the spin-parity $J^{\mathrm{P}} = (3/2)^{+}$ baryon decuplet.


doi.org/10.32388/ZM7QNO

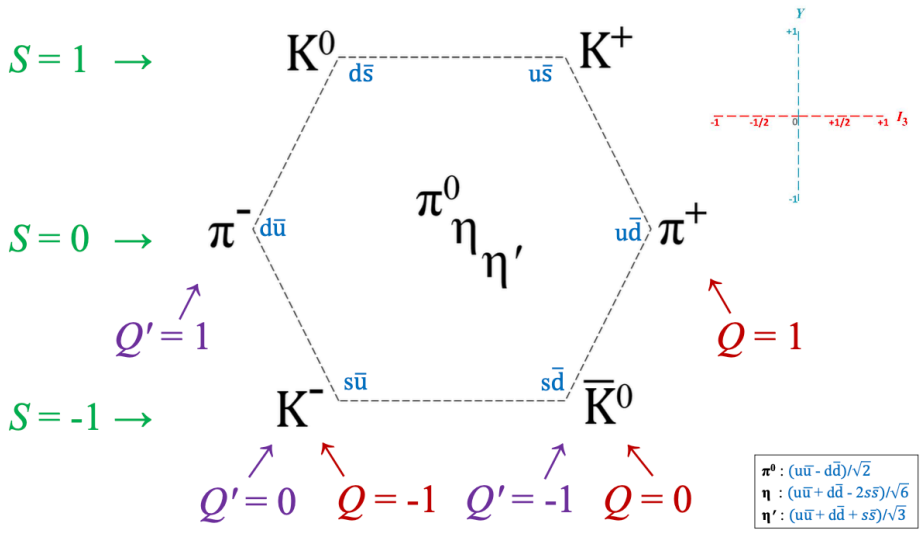


**Figure 3.** The weight diagram of the spin-parity $J^{\mathrm{P}} = 0^{-}$ pseudoscalar meson nonet.

## 2. Particle rest-masses, mass deficits, and their binding factors

Particle rest-masses ($M$) and mass deficits ($MD$) are listed in Tables 1-3 for baryons and mesons. All mass-related values are given in MeV. Quantities on the right of the broken vertical lines are derived from the data on the left of these lines.


doi.org/10.32388/ZM7QNO

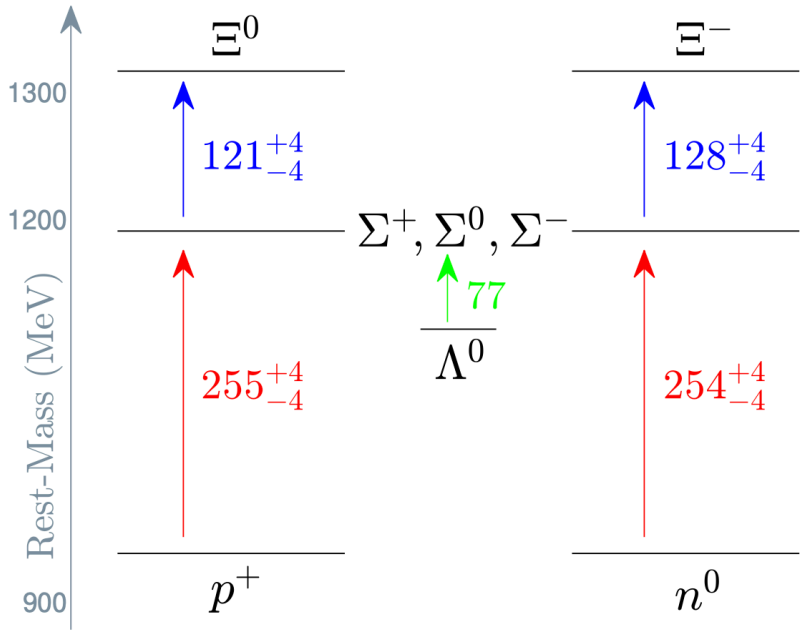


**Figure 4.** Average rest-mass energy levels for the $J^{\mathrm{P}} = (1/2)^+$ baryons of Figure 1.

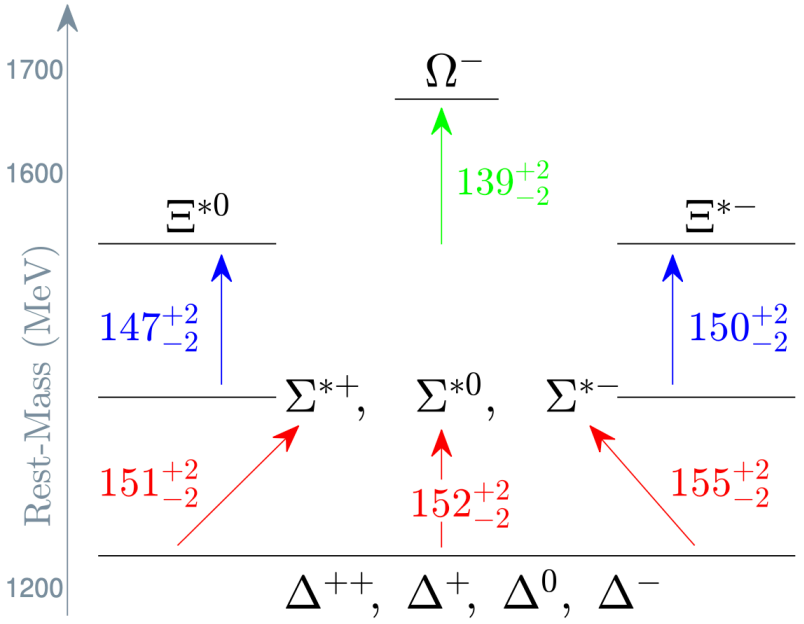


**Figure 5.** Average rest-mass energy levels for the $J^{\mathrm{P}} = (3/2)^+$ baryons of Figure 2.


doi.org/10.32388/ZM7QNO

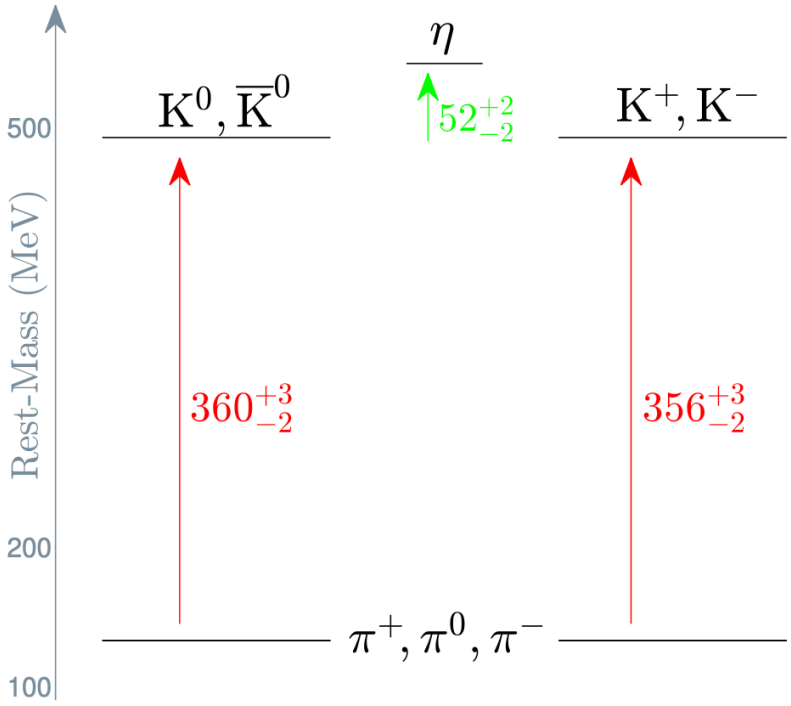


**Figure 6.** Average rest-mass energy levels for the $J^{\mathrm{P}} = 0^-$ pseudoscalar meson nonet of Figure 3. The massive particle $\eta'$ is off scale; it lies 410 MeV above $\eta$ which, in turn, lies 410 MeV above the pions. Also not shown, the excitations $\mathrm{K}^{*\pm}$ and $\mathrm{K}^{*0}$ lie 398 MeV above $\mathrm{K}^{\pm}$ and $\mathrm{K}^0$, respectively.

### *2.1. Rest-mass jumps between particle groups*

In Tables 1-3, the very few masses not yet measured by experiment, but predicted by the Standard Model (SM) [4], are listed in parentheses. It may not be as obvious in these listings, but rest-masses of the low-energy states are effectively quantized in each of the three tables, although the rules differ between groups.

The weight diagrams of the low-energy states are shown in Figures 1-3, and the average quantization rules are shown in Figures 4-6. The detailed distributions of all individual energy jumps between states are quite crowded in all cases; they are shown in Appendix A (Figures A1-A3). The approximate energy jumps delineated from the data with increasing rest-energy are as follows:

1. $J^{\mathrm{P}} = (1/2)^+$ baryons: 256 MeV and 128 MeV (Figures 4 and A1); although the ~120-MeV jump to $\Xi^0$ may be subject to a slightly different rule; also, the decay $\Sigma^0 \to \Lambda^0 \gamma$ always emits a 77-MeV

photon ($\gamma$), an important result that allows us to investigate below the isospin content of $\Sigma$ baryons.

2. $J^{\mathrm{P}} = (3/2)^{+}$ baryons: 150 MeV for all three jumps (Figure 5 and A2); although the ~140-MeV jump to $\Omega^{-}$ may be subject to a slightly different rule.
3. $J^{\mathrm{P}} = 0^{-}$ pseudoscalar mesons: 360 MeV and 50 MeV (Figure 6 and A3); the high-energy state $\eta'$ (not shown) lies 410 MeV above $\eta$, which in turn lies 410 MeV above the pionic ground state.
4. $J^{\mathrm{P}} = 1^{-}$ vector mesons ($\rho \to \mathrm{K}^{*} \to \phi$): 120 MeV in both jumps (see Table 3).

## *2.2. Mass deficits and binding factors*

Mass deficits and binding factors are listed in Tables 1-3 in columns *MD* and *BF*, respectively. *MD* values were obtained from the rest-masses by subtracting the masses of the valence (anti)quarks (quark masses are listed in Table 4 below).

*BF* values were calculated from the corresponding *MD* values by assuming that (a) each (anti)quark is bound by a "deficit" of rest-energy proportional to its own rest-mass; (b) the scale factor *BF* is the same for all (anti)quarks confined in each particle; and (c) the relative factor of $\vartheta_{\mathrm{e}} = 2$ in the electric charges of the (u, c, t) (anti)quarks is taken into account. Without the latter assumption, the *BF* values of the u and c quarks and their antiquarks would double and the *BF* patterns seen in Tables 1-3 would not surface; in particular, the *BF* values would not be characteristically the same within each particle group.

As a case study, we describe the *BF* calculations for the nucleons, and we show how assumption (c) came into being: Initially, we set up two equations for the *MD*s of the nucleons, and we solved the system of equations to obtain the corresponding $BF_{\mathrm{s}}$. The two equations are

$$\begin{aligned} \text{Proton (uud)}: &\quad 2m_{\mathrm{u}}\, BF_{\mathrm{u}} + \ m_{\mathrm{d}}\, BF_{\mathrm{d}} = MD_{\mathrm{p}} \\ \text{Neutron (udd)}: &\quad m_{\mathrm{u}}\, BF_{\mathrm{u}} + \ 2m_{\mathrm{d}}\, BF_{\mathrm{d}} = MD_{\mathrm{n}} \end{aligned} \tag{1}$$

where $m_{\mathrm{q}}$ is the mass of quark q (u or d) and the $MD$ values for the proton and the neutron are $MD_{\mathrm{p}} = M_{\mathrm{p}} - 2m_{\mathrm{u}} - m_{\mathrm{d}}$ and $MD_{\mathrm{n}} = M_{\mathrm{n}} - m_{\mathrm{u}} - 2m_{\mathrm{d}}$, respectively. The two $BF_{\mathrm{q}}$ values of the solution are different and seemingly unrelated ($BF_{\mathrm{u}} = 143.6$ and $BF_{\mathrm{d}} = 66.16$), but when the fraction ($f$) of the constituent mass corresponding to each quark is calculated, the result is exactly $f = 1/3$ for all three quarks in both nucleons. This congruence implies that the above equations can be solved individually for a single (particle) binding factor, scaling of course each of the u quarks according to assumption (c). We then solve the equation

$$(2\vartheta_{\mathrm{e}} m_{\mathrm{u}} + m_{\mathrm{d}})\, BF_{\mathrm{p}} = MD_{\mathrm{p}}\,, \tag{2}$$

for the proton scale $BF_{\mathrm{p}}$, and the equation

$$(\vartheta_{\mathrm{e}} m_{\mathrm{u}} + 2m_{\mathrm{d}})\, BF_{\mathrm{n}} = MD_{\mathrm{n}}\,, \tag{3}$$

for the neutron scale $BF_{\mathrm{n}}$, where the electric-charge factor

$$\vartheta_{\mathrm{e}} = 2\,, \tag{4}$$

is applicable to u and c quarks (also to the t quark, which however is too massive to be confined in hadrons; see Table 4 below); and we obtain $BF_{\mathrm{p}} = 69.82$ and $BF_{\mathrm{n}} = 67.94$. The small difference between these $BF$s is, in part, due to the slightly higher $MD$ of the proton ($MD_{\mathrm{p}} - MD_{\mathrm{n}} = 1.22$ MeV), a value that is not nearly as well-known as the difference in nucleonic masses ($M_{\mathrm{p}} - M_{\mathrm{n}} = -1.29$ MeV). We analyze these oppositely-signed differences in § 3 below.

## *3. Coulomb-repulsion origin of mass-deficit difference in nucleons and pions*

We adopt an elementary model of valence (anti)quark charges confined inside a particle, and we calculate the potential of the repulsive Coulomb-force components to do work, if they were not suppressed in the bound state. Naturally, these repulsions are neutralized by work done by the strong force, which then constantly contributes an equal amount of energy to the $MD$ of the particle. Attractive forces are ignored because they are not working to disrupt the particle.[1] The associated kinetic-energy content due to attractive forces is of course included in the $MD$s along with the energy of the binding gluonic field and additional dynamical contributions from the so-called quark condensate and QCD trace anomaly [5][6][7].

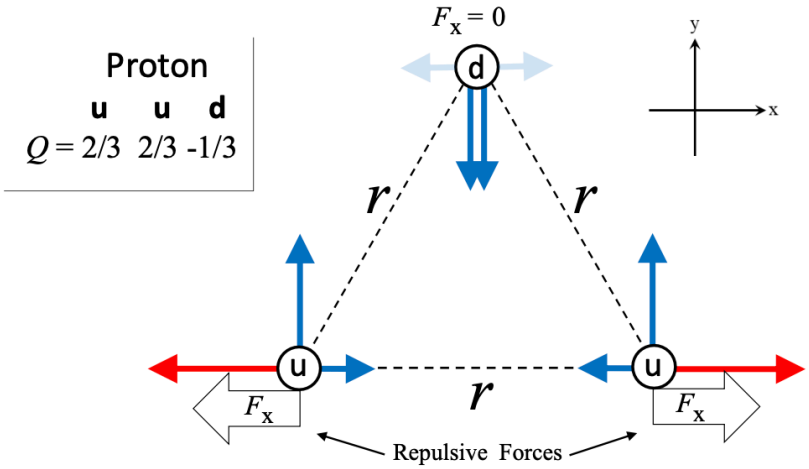


**Figure 7.** Repulsive Coulomb forces $F_x$ between the $Q = +2/3$ u quarks in the proton. The relative magnitudes of the forces are drawn to scale $(1 : \sqrt{3} : 2)$. Such repulsion does not develop between the $Q = -1/3$ d quarks in the neutron (Figure 8), which results in a higher mass deficit for the proton (+1.2167 MeV; top of Table 1). Typical distance $r$ is assumed to be the same as the charge radius of the proton [8][9][10][11][12].

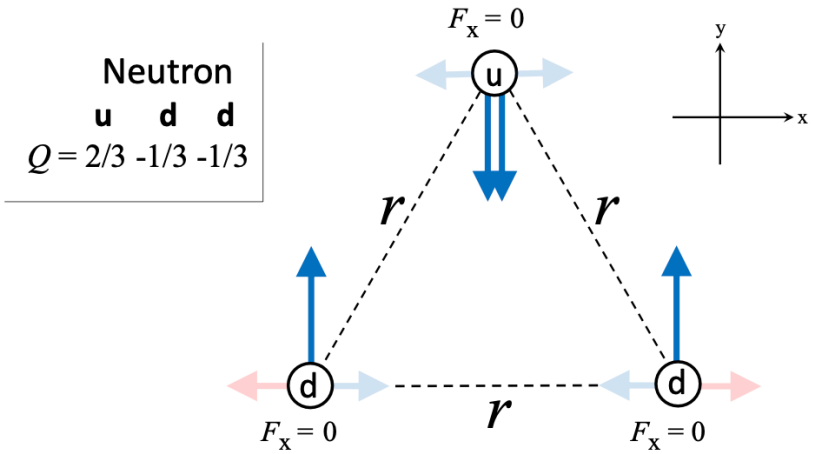


**Figure 8.** No repulsive Coulomb forces between the $Q = -1/3$ d quarks in the neutron, such as those between the u quarks in the proton (Figure 7). The relative magnitudes of the forces are drawn to scale $(1 : \sqrt{3})$. Typical distance $r$ is assumed to be the same as the charge radius of the proton [8][9][10][11][12].


doi.org/10.32388/ZM7QNO

We find that the simple electrostatic model shown in Figures 7-9 below describes to a large extent the small differences in the known $MD$s only in nucleons and pions (§ 3.1 and § 3.2, respectively). All other states are highly energetic while they last, and the work done by the strong field against the repulsive Coulomb forces is just a small fraction of the corresponding $MD$ differences. True to form, we demonstrate in § 3.3 that Coulomb repulsion alone does not explain fully the measured $MD$ differences in $\Sigma^-/\Sigma^0$ baryons with $MD$ values ~1090 MeV, differing by only 2.30 MeV; and in $\Xi^-/\Xi^0$ baryons with $MD$ values ~1130 MeV, differing by only 4.34 MeV (Table 1 and Appendix B).

### *3.1. Nucleons*

The Coulomb forces between quarks in the proton and the neutron are drawn to scale in Figures 7 and 8, respectively. Faint arrows indicate components that cancel out. There are no repulsive components in the neutron. The resultant repulsive forces $F_x$ in the proton are depicted by thick arrows.

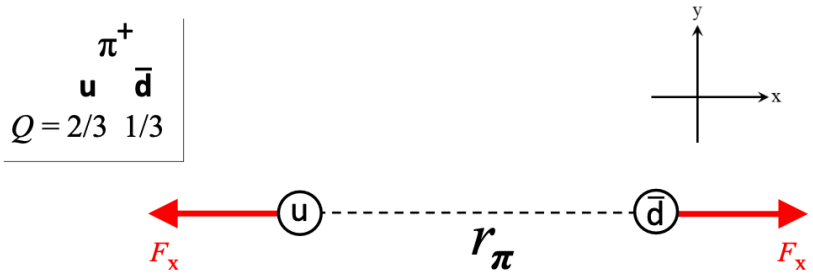


**Figure 9.** Repulsive Coulomb forces $F_x$ between the u and $\bar{d}$ quarks in pion $\pi^+$. Such repulsion does not develop in the mixed $\pi^0$ state $(|u\bar{u}\rangle - |d\bar{d}\rangle)/\sqrt{2}$, which results in a higher mass deficit for the $\pi^\pm$ pions (+4.59 MeV; top of Table 3). Typical distance $r_\pi$ is much smaller than the charge radius of the proton [13], and it is discussed in the text.

For the characteristic side length $r$ of the equilateral triangle shown in Figure 7, we adopt the charge radius of the proton [8][9][10][11][12], so that $r = 0.83$ fm (where 1 fm $= 10^{-15}$ m). Then we find from Coulomb's law that $F_x \simeq 112$ Cb. The work that could be done by these two forces over distance $r$ in the proton then is

$$W_p = 2rF_x \simeq 1.16 \text{ MeV}, \tag{5}$$

accounting for 95% of the $(MD_p - MD_n)$ difference of 1.22 MeV seen in Table 1.

### 3.2. Pions

The repulsive Coulomb forces between the u and $\bar{\mathrm{d}}$ quarks in the positively charged pion $\pi^+$ are shown in Figure 9. The same forces also appear in $\pi^-$, but not in the neutral state $\pi^0$. In Figure 9, distance $r_\pi$ between the quarks is taken to be the characteristic radius of the pion which is not known [13]. The problem is that the charge radius of $\pi^\pm$ (0.66 fm) is mostly due to a dominant $\rho^0$-resonance (intervening in the annihilation process $e^+\,e^- \rightarrow \gamma \rightarrow \pi^+\,\pi^-$) that also affects the size of the proton, but not nearly as much (Refs. [13], Chapter 1, and [14]).

So, we need to estimate the typical distance $r_\pi$ between the quark and the antiquark in $\pi^\pm$ pions, and this determination requires some new assumptions. First, it is not reasonable to scale the nucleons down to the pions by assuming that the energy density of the binding field is the same in the two states. This is because the pions are quite different and much smaller than all other hadrons--the lowest-energy excitation of the vacuum [13] and a ground state for the mesons. (Such an attempt would yield a large radius of 0.44 fm, which is not acceptable.) On the other hand, the pions contain only two point-like quarks that are presumably connected by a string in modern theories at the intersection of QCD and superstring theory [15][16][17][18][19][20]. Then, it seems reasonable to assume that it is the *mass per unit length* between two (anti)quarks that is about the same in nucleons and pions. With this assumption, we find that $r_\pi = 0.125$ fm in Figure 9 and, from Coulomb's law, that $F_\mathrm{x} \simeq 3300$ Cb. The work that could be done by these two forces over distance $r_\pi$ in the charged pions then is

$$W_{\pi^\pm} = 2 r_\pi F_\mathrm{x} \simeq 5.14\ \mathrm{MeV}, \tag{6}$$

i.e., 12% larger than the $(MD_{\pi^\pm} - MD_{\pi^0})$ difference of 4.59 MeV seen in Table 3. The disagreement is entirely due to our rough estimate of $r_\pi$; and it would go away for an ad hoc value of $r_\pi = 0.14$ fm.

### 3.3. $\Sigma^-/\Sigma^0$ and $\Xi^-/\Xi^0$ baryons

The $\Sigma^\pm$ baryons are charged excitations of the nucleons ($\Sigma^\pm \rightarrow n^0\,\pi^\pm$ and $\Sigma^+ \rightarrow p^+\,\pi^0$) [1][2]. In contrast, the $\Sigma^0$ baryon is an excitation of the $\Lambda^0$ resonance ($\Sigma^0 \rightarrow \Lambda^0\,\gamma$), which is itself a nucleonic excitation. Although the $\Sigma^+/\Sigma^0 MD_\mathrm{s}$ are comparable (Table 1), $MD_{\Sigma^+} < MD_{\Sigma^0}$ by 0.76 MeV. [2] On the other hand,

$$MD_{\Sigma^-} - MD_{\Sigma^0} = 2.30\ \mathrm{MeV}. \tag{7}$$

This difference is not mostly the result of suppression of repulsive Coulomb forces between the dds valence quarks in $\Sigma^-$ (the uds quarks in $\Sigma^0$ do not develop repulsive forces in our simple model, just as is

shown in Figure 8 for the neutron). We demonstrate this by estimating the work that could be done in $\Sigma^-$ over distance $r$ by the three repulsive forces $F_{\rm R}$ between the dds quarks (all Coulomb forces are repulsive since all charges are negative).

We adopt again the simple triangular baryonic configuration as in § 3.1. Since $\Sigma^-$ is a nucleonic excitation, we adopt $r = 0.83$ fm here as well. (Scaling based on equal linear mass densities would produce 1.06 fm and a smaller Coulombic contribution to the *MD* difference.) With these assumptions, we find that $F_{\rm R} \simeq 64.5$ Cb for the repulsive Coulomb force at each vertex of the equilateral triangle. The work that could be done by these forces over distance $r$ in the $\Sigma^-$ baryon then is

$$W_{\Sigma^-} = 3rF_{\rm R} = 1.00 \text{ MeV}, \tag{8}$$

which is only 43.5% of the *MD* difference shown above in equation (7).

The above estimates also apply to the $\Xi$ baryons (excitations of $\Lambda^0$ with $MD_{\Xi^-} - MD_{\Xi^0} = 4.34$ MeV; Table 1), in which the three $\Xi^-$(dss) valence quarks carry the same negative charge as the dds quarks in $\Sigma^-$; whereas $\Xi^0$(uss) shows no repulsive Coulomb forces in this model. Thus, $W_{\Xi^-} = 1.00$ MeV (as in equation 8 for $\Sigma^-$), and this amounts to only 23% of the measured *MD* difference of 4.34 MeV.

The results described in this section allow for a deep and thorough examination of the energy content of the $\Sigma$ and $\Xi$ excitations from the nucleonic ground state and the $\Lambda^0$ resonance, respectively. We have included a detailed analysis in Appendix B.

## 4. The strong charge $Q'$

The third component $I_3$ of the isospin $I$ and the hypercharge $Y$ (Tables 1-3) are conserved in strong interactions (see also § 5 for examples). These values are related to the always conserved EM charge $Q$ by the NNG formula [21][22][23]

$$Q = Y/2 + I_3. \tag{9}$$

Unlike $Q$, the hypercharge $Y$ is not an actual EM charge, since this equation involves also the $I_3$ isospin component. The next question then is, what do we get in place of $Q$ when we flip the sign of $I_3$ in equation (9)? Apparently, we get a supplementary charge $Q'$ such that

$$Q' \equiv Y/2 - I_3, \tag{10}$$

and then we find by adding equations (9) and 10) that

$$Q + Q' = Y. \tag{11}$$

So, $Q'$ is the supplement of $Q$ in strong interactions; and it is independent of the EM charge $Q$, unlike the hypercharge $Y$.

The charges $Q$ and $Q'$ are true opposites only for the following *charged* $Y = 0$ *particles*: $\Sigma^{\pm}$ and $\Sigma_b^{\pm}$; $\Sigma^{*\pm}$ and $\Sigma_b^{*\pm}$; and $\pi^{\pm}$ and $\rho^{\pm}$ (Tables 1-3). All other $Y = 0$ particles are at the centers of their weight diagrams, and they have $Q = Q' = 0$ (e.g., $\Sigma^0$, $\Sigma^{*0}$, and $\pi^0$ in Figures 1-3-). In the general case with $Y \neq 0$, the strong charge $Q'$ is *the translation of the EM* $Q$ across the $Y$-axis (where $I_3 = 0$).

The strong charge $Q'$ is conserved in strong decays, in which both $Y$ and $I_3$ are also conserved individually (see § 5 for a classification of strong/EM versus weak decays, based on $Q'$). We finally rewrite equation (11) (and we calculate $Q'$ in Tables 1-4) in the convenient form

$$Q' \; = \; Y - Q \, , \tag{12}$$

with the stipulation that $Q'$ is equivalent to either one of the well-known quantum numbers $(Q, I_3, Y)$ governing the strong and EM interactions. Finally, we identify $Q'$ as the quantum number that remains constant along the *right-leaning sides/diagonals* in the weight diagrams depicted in Figures 1-3 above.

It may seem that $Q'$ is redundant, but it is not. We describe two examples that show its efficacy:

a. In some kaon decays, $\mathrm{K}^{\pm}$ and $\mathrm{K}^0/\overline{\mathrm{K}}^0$ can produce three pions via the reactions $\mathrm{K}^{\pm} \to \pi^+\pi^-\pi^{\pm}$ and $\mathrm{K}^0/\overline{\mathrm{K}}^0 \to 3\pi^0$, respectively [1][2]. The only quantum number that differentiates charged from neutral kaon decays is $Q'$, which switches from $0 \to \pm 1$ and from $\pm 1 \to 0$, respectively (see Table 3). No other quantum number can capture such oppositely-directed transitions in these two types of weak decays of the K-triplet. We revisit kaon decays in Appendix B and Appendix C below.
b. In quarks (Table 4), $Q'$ is the only quantum number (among EM, strong, and weak numbers) that exhibits a repetitive $Q' = (-1/3, +2/3)$ symmetry with increasing quark mass in each generation. This is a notable property, especially since, for EM charge $Q$, the $(-1/3, +2/3)$ pattern breaks down in first-generation (u, d) quarks.

Another example demonstrating an inconspicuous property of the strong charge $Q'$ is described in context in § 5.6 below.

## 5. Strong/EM decays based on $Q'$ conservation

In this section, we delineate the strong/EM decays by monitoring the strong charge $Q'$ (instead of using $I_3$ or $Y$) throughout several common and unusual decays of baryons and mesons, in which the EM

charge $Q$ is of course always conserved. When $Q'$ is conserved, the well-known numbers $I_3$ and $Y$ are automatically conserved as well (yet they cannot distinguish strong from EM decays without help from total isospin $I$, which is not conserved in EM decays).

This one-parameter $Q'$-classification singles out the weak interactions too, just as $Y$ or $I_3$ commonly do. Below, we use $Q'$ to separate first the weak decays from all other decays; then, we formulate an additional distinction that $|Q - Q'|$ offers which appears to be capable of separating strong from EM decays.

### *5.1. $J^{\mathrm{P}} = (1/2)^+$ baryon octet*

These baryons are listed at the top of Table 1 and illustrated in Figure 1. Here we show in Table 5 their strong/EM decays in which $Q'$ is conserved. We also categorize their excited and resonant states in the notes.

### *5.2. $J^{\mathrm{P}} = (3/2)^+$ baryon decuplet*

These baryons are listed at the top of Table 2 and illustrated in Figure 2. Here we show in Table 6 their strong/EM decays in which $Q'$ is conserved. We also categorize their higher-energy states in the notes.

### *5.3. $J^{\mathrm{P}} = 0^-$ pseudoscalar meson nonet*

These mesons are listed at the top of Table 3 and illustrated in Figure 3. Here we show in Table 7 their strong/EM decays in which $Q'$ is conserved. We also categorize their excited and resonant states in the notes.

### *5.4. $J^{\mathrm{P}} = 1^-$ vector meson nonet*

The vector mesons are listed at the bottom of Table 3. Here we show in Table 8 some typical strong/EM decays of the SU(3) nonet [1][2] in which $Q'$ is conserved. This group contains particles such as $\rho, \Phi, \omega$, and K*. We also categorize their higher-energy states in the notes.

### *5.5. Summary of Tables 5-8*

We summarize the material in Tables 5-8 as follows:

1a. The $J^{\mathrm{P}} = (1/2)^+$ baryon octet shows virtually no strong decays. Only $\Sigma^0$(uds) decays via photon emission (pions are not produced), and the proton does not decay at all. All other decays are due to weak interactions, and they all characteristically produce pions or leptons (see top of Table 5).

1b. Higher-energy $J^{\mathrm{P}} = (1/2)^+$ baryon states do reveal strong interactions, except $\Lambda_c^+$(udc) and $\Omega_c^0$(ssc) (see bottom of Table 5). On the other hand, $\Lambda_b^0$(udb) shows both types of decay in different channels (see notes in Table 5).

2. The $J^{\mathrm{P}} = (3/2)^+$ baryons all show strong decays, except one, the $\Omega^-$(sss) excitation (Table 6) which also exhibits some unique properties (strangeness $S = -3$, $Y = -2$, $I = 0$), but not an unusual value of $Q' = -1$ (see Table 2).

3a. In the $J^{\mathrm{P}} = 0^-$ meson group, the pions show strong/EM decays, but the kaons show only weak decays (Table 7). At higher energies, the D and B mesons show very few strong/EM decays.

3b. In the $J^{\mathrm{P}} = 1^-$ group, all vector mesons with rest-masses below 1020 MeV show strong/EM decays (Table 8). At higher energies, the decays are all strong/EM as well, with the striking exception of $\mathrm{D}_*^+(\mathrm{c}\bar{s})$ which exhibits two uncommon properties ($Y = +2$, $I = 0$), but not unusual values of $S = +1$ and $Q' = +1$ (see Table 3).

### *5.6. Electromagnetic versus strong decays*

It is generally stated that EM decays do not conserve total isospin $I$, which distinguishes them from strong decays [24][25]. Although this statement is essentially correct, the implied separation is imprecise and needs to be refined (by monitoring $Q'$ instead of $I$), as there are few decays that get misclassified by total isospin:

a. Decays of the type $\rho \to \pi\pi$ (where $Q = 0 \to 0\,0$ is the only one not allowed) are said to be strong [24], although total isospin is clearly not conserved (all three particles have $I = 1$; Table 3)).

b. Decays of the $\Delta$-baryons are said to be strong [24], as they all conserve total isospin. But $\Delta^+$ and $\Delta^0$ each show two decay channels, so it becomes hard to argue that somehow the strong force cannot settle into one preferred mode of decay in driving these resonances back to their ground states.

We revisit these exceptional cases in § 5.6.2 below, where we apply a new methodology based on $|Q - Q'|$ that we develop in § 5.6.1.

#### *5.6.1. The important role of $|Q - Q'|$.*

EM charge $Q$ is conserved in all hadron decays, signifying that EM forces are always present in particle reactions. Here, we search the 31 strong/EM decays listed in Tables 5-8, and we identify the predominantly EM decays based only on the behavior of the strong charge $Q'$ (along with the always

visible EM charge $Q$); that is, without relying on the (non)conservation of isospin $I$ at all. The resulting classification of reactions is summarized in the 3 cases listed in Table 9.

The EM versus strong classification scheme in Table 9 stems from the following principle: Eliminating $Y$ between equations (9) and (10), we determine $I_3$ in terms of the difference between the two charges, viz.

$$I_3 = \frac{1}{2}(Q - Q')\,, \tag{13}$$

which of course shows that $I_3$ is conserved in strong and EM decays, in which the two charges are conserved. But predominantly strong interactions should require, in addition, the conservation of the magnitude $|I_3|$, a number that is not conserved in EM interactions In effect, we disregard here the term $\left(I_1^2 + I_2^2\right)$ that is not fully deterministic (by the Uncertainty Principle) when a (strong) state has a definite value of the $I_3$ component [26]. Therefore, the two types of non-weak decays should be distinguishable based on $|I_3|$ alone. To this end, the factor of 1/2 in equation (13) is not needed, which allows us to finally monitor only the "distance" between the two charges, viz.

$$|Q - Q'| \;\equiv\; \sqrt{(2I_3)^2}\;, \tag{14}$$

in the 31 examples of strong/EM decays listed in Table 9.

In Table 9, the decays grouped together in Cases 2 and 3 (predominantly strong and predominantly EM decays, respectively) are classified on the basis of nonzero $|Q - Q'|$ values precisely as would also be expected from the (non)conservation of $I$. On the other hand, the EM decays of Case 1 (with $|Q - Q'| \equiv 0$ across each reaction) hold some surprises:

a. Reactions emitting photons reveal a primarily EM nature, and so do reactions emitting neutral vector mesons ($\omega$, $\phi$, or $J/\psi(1s)$; but not $\Upsilon(1s)$ whose enormous 9.46-GeV rest-mass trumps all the other particles).
b. By showing their true EM nature, reactions with $|Q - Q'| \equiv 0$ (i.e., $I_3 \equiv 0$) teach us that in cases where $I_3 = 0$ across the entire decay reaction (i.e., $Q = Q' = Y/2$), (non)conservation of $I$ becomes practically irrelevant, and then the reaction is mediated primarily by the EM interaction.
c. The decay $\Lambda_b^0 \to \Lambda_c^+ D_s^-$ produces a charged meson and a $\Lambda_c^+$, the only $\Lambda$-particle that actually carries EM charge. This EM reaction also shows that $Q' = 0 \to 1$ -1 = 0, which differentiates it from (i) the other $Q' = 0 \to 0\,0 = 0$ EM decays producing photons (Case 1); and (ii) the $\Lambda$-producing $\Sigma^*$ and $\Sigma_c$ decays mediated by the strong interaction (Case 2).

The decay $\Lambda_b^0 \to \Lambda_c^+ D_s^-$ in item (c) represents one of many cases in which two opposite EM charges ( $Q = 0 \to 1$ -1) appear "out of nowhere" in the decay fragments; thus, the reaction must be characterized as naturally EM, irrespective of the behavior of its quantum numbers (although the weak force may have a role too in intermediate steps). On the other hand, $I = 0 \to 0\,0$, indicating that isospin conservation is not relevant here; an attempt to use "$I$-conservation" for $I \equiv 0$ across the reaction would lead to misclassification. Another conundrum appears in 2 of 6 $\Delta$-baryon decay channels which we examine below.

### *5.6.2. Decay channels of $\rho$ and $\Delta$ resonances.*

(a) Based on the $|Q - Q'|$ criterion, the primary modes of $\rho^{\pm}$ are strong (ST), but the decay of the neutral $\rho^0$ to charged pions is EM (Table 9). Since $Y = 0$ for all particles involved, then $Q' = -Q$, thus the strong charge is obviously conserved in all of these decays. But the charge distance $|Q - Q'| = 2|Q|$ is not conserved in the ubiquitous decay $\rho^0 \to \pi^+ \pi^-$ (Case 3 in Table 9).

(b) The decays of $\Delta^{++}$ and $\Delta^-$, as well as the primary decays of $\Delta^+$ and $\Delta^0$ down to their parental states ($p^+$ and $n^0$, respectively), are all mediated by the strong interaction (Case 2 in Table 9; [24][25]), and they are not going to occupy us further. On the other hand, $\Delta^+$ and $\Delta^0$ have two additional decay channels in which they do not return to their parental states, viz.

$$\Delta^+ \to n^0\,\pi^+ \,(I = \tfrac{3}{2} \to \tfrac{1}{2} \to \mathrm{ST};\ |Q - Q'| = 1 \to 12 \Rightarrow \mathrm{EM}), \tag{15}$$

and

$$\Delta^0 \to p^+\,\pi^- \,(I = \tfrac{3}{2} \to \tfrac{1}{2} \to \tfrac{1}{2} \to \mathrm{ST};\ |Q - Q'| = 1 \to 12 \Rightarrow \mathrm{EM}). \tag{16}$$

By $I$-conservation, these two reactions are thought to generally belong to the ST category, where all the other $\Delta$-decays also belong; but $|Q - Q'|$ in equations (15) and (16) disagrees and places them in the EM category.

Channel (15) cannot be judged at first sight, but channel (16) is yet another example of EM charges appearing "out of nowhere" in the two fragments. Thus, we suggest that these two decays are mediated primarily by the EM interaction (unlike the strong decays $\Delta^+ \to p^+\,\pi^0$ and $\Delta^0 \to n^0\,\pi^0$); and that the (non)conservation of the charge distance $|Q - Q'|$ (equation (14)) is the refinement needed to distinguish accurately between primarily EM and ST decays.

# 6. Summary and open questions

## *6.1. Summary*

In this work, we have carried out a meta-analysis of some of the extensive hadron data painstakingly collected by the Particle Data Group [1][2] over many years. In § 2, we examined the rest-masses and the mass deficits of the hadrons. We found that jumps in rest-masses appear to be approximately quantized, and that mass deficits can be reconstructed from the masses of the valence quarks multiplied by the same binding factor in each hadron. We summarized our results in Figures 4-6 and in Tables 1-3, respectively.

In § 3, we showed that small differences in the mass deficits of nucleons or pions (the identified ground states of baryons and mesons, respectively) can be explained by suppression of the repulsive Coulomb forces by the strong field that binds these fundamental particles together in a highly dynamical environment. The mass-deficit differences of higher excitations and resonances cannot be explained in the same way; such higher energetic states are in possession of much more free energy (while they last) than that predicted by suppression of Coulombic repulsions.

In § 4, we introduced a (long-overdue) charge, the "strong charge" $Q'$; quantum number $Q'$ is not a real charge (the strong field is charge-blind), it is just an imitation that describes the weight of the strong force among the various well-known quantum numbers, such as $Q$, $I_3$, and $Y$. We discovered $Q'$ in the preeminent weight diagrams of low-energy hadrons (Figures 1-3) by asking an obvious (and long-overdue) question: which quantity remains invariant along the right-leaning sides and digonals of the geometric figures depicted in these weight diagrams? The answer was the strong charge $Q' = Y - Q$ (equation (12)), a _translation_ of the EM charge $Q$ across the ($I_3 = 0$) $Y$-axis, where $I_3$ is the third component of isospin $I$ and $Y$ is the hypercharge.

Based on the results presented in § 5, the strong charge $Q'$ is expected to have a long life with us: not only is it as tall a peer to $Y$ and $I_3$ (equation (10)) in separating weak from strong/EM particle decays, but it can also help us distinguish predominantly strong from EM decays with a little help from the (always visible in reactions) EM charge $Q$ (quantum number $|Q - Q'|$ in equation (14)).

We have deferred additional tortuous analyses to three appendices. In Appendix A, we present transition diagrams between the various excitations and resonances of the low-energy particles (Figures 13-13).

They appear to be too crowded to the eye, and this is why we also drew collective, summarizing diagrams in Figures 4-6 above.

In Appendix B, we calculate the transition energies between valence states in $\Sigma/\Lambda^0/\Xi/\Omega/\Xi^*$ baryons at the quark level. We determine the energy cost for lower-mass quarks (u, d, s) to transform to different quarks via the weak interaction. Perhaps the most important result is not the numerical values obtained for the various quark transitions (see, e.g., equation (15)), but the realization that an isospin change by $\delta I = +1/2$ does not carry the same cost during the $I = 0 \to 1/2$ and $I = 1/2 \to 1$ transitions. In a quantum state with $I = 0$, isospin is not realized, and the $I = 0$ particle needs to be "paid" (a small amount of excitation energy) to be taught of the existence of nonzero isospin; thus, $I_{0\to 1/2} \gtrsim I_{1/2\to 1}$. By the same token, when $I_3 \equiv 0$ across a decay reaction (Case 1 in Table 9), the quantum states cannot possibly conserve zero isospin, a quantity that is obviously not present in the reaction.

In Appendix C, we turn to antimatter quarks in low-energy K and $\pi$ pseudoscalar mesons. We calculate the antiquark transition energies, and we find, to our surprise, that they are very different from the quark energy levels in ordinary matter (Appendix B). In particular, we determine that $\bar{\mathrm{d}}$ is the lowest antiquark state (i.e., the ground state), as opposed to the well-known u-quark ground state in ordinary matter. The resulting (anti)quark transition diagrams are depicted side-by-side in Figure 13 for comparison purposes. As we discuss below, the results in this appendix form a basis for understanding the origin of CP violation.

### *6.2. Open questions*

Examining the main results of this meta-analysis, we do not see any obvious questions left open-ended for the future. Except possibly the minor disagreement over the basics between $I$- and $|Q - Q'|$-conservation (see § 5.6.2.) in the two alternative channels of $\Delta^+/\Delta^0$ decays; this issue deserves some more consideration in the near future.

On the other hand, we are wrapping up this investigation, thinking about some additional not-so-obvious open questions. Briefly, these are:

1a. Consider the binding factors ($BF$) of the nucleons listed at the top of Table 1 ($BF = 69.8$ and $67.9$ for $p^+$ and $n^0$, respectively). Their sum, $137.7$, is close (to within $0.5\%$) to the reciprocal of the EM fine-structure constant $\alpha = 1/137.036$[3], i.e., the famous number $\alpha^{-1} \simeq 137$[27][4]. Then, the average binding factor $\overline{BF}_{\mathrm{q}} = 68.85$ of each quark in each nucleon appears to be very close to

$$\frac{\alpha^{-1}}{2} = 68.52\,. \tag{17}$$

1b. Consider also the binding factors ($BF$) of the pions listed at the top of Table 3 ($BF = 14.8$ for $\pi^{\pm}$). This $BF$ value is close (to within $0.4\%$) to half of the reciprocal of the weak interaction coupling constant $\alpha_{\rm w}$ (i.e., $\alpha_{\rm w}^{-1}/2$), where

$$\alpha_{\rm w} = \frac{{g_{\rm w}}^2}{4\pi} = \frac{1}{29.47}\,, \tag{18}$$

evaluated from the gauge factor $g_{\rm w} = 0.653$[4] of the weak interaction. It seems unavoidable that the fundamental coupling constants of the subatomic interactions are correlated with the binding factors of the ground states, the nucleons and the pions.

2a. The above identifications are also supported, to an extent, by the constituent quarks of the $\Delta$-baryons which show the largest by far $BF$ values among all elementary particles (Table 2). Their average binding factor $\overline{BF}_{\rm q} = 90.7$ for each individual quark is smaller only by $0.7\%$ than the value

$$\frac{4}{3}\left(\frac{\alpha^{-1}}{2}\right) = 91.36\,. \tag{19}$$

For the $BF$ values of these low-lying resonances (just 293 MeV above the nucleons), the ST-factor of $4/3$ appears to be necessary in the rescaling of the EM factor of $\alpha^{-1}/2$ (equation (17)).

2b. We have identified the above ST-factor of $4/3$ with the quadratic Casimir charge $C_F$ of the SU(3) fundamental representation [3] [28]. So, it seems by extension that all $BF$'s listed in Tables 1-3 are related in multifarious ways to the fundamental QCD couplings and their gauge factors [4][28]. In such a case, the $BF$ value for each particle reveals information about the constituent subatomic fields that support the current quarks and antiquarks in the dynamical environments they create.

3. The small differences in $BF$ values within the same state (or group of particles) are significant. They seem to be caused by the components of the strong field and the particular ways they use to keep each individual particle together (or not at all, in cases in which the $BF$ values are identical within the group; Tables 1-3). This conclusion stems from the following astonishing congruence: the precise $BF$-ratios of the $\Delta$-baryons and the nucleons are equal, viz.

$$\frac{BF(\Delta^+)}{BF(\Delta^0)} = \frac{BF(p^+)}{BF(n^0)} = 1.028\,; \tag{20}$$

and the pionic ratio $BF(\pi^+)/BF(\pi^0) = 1.033$ is not too different, although the value of $BF(\pi^0)$ is just an approximation obtained for the mixed neutral state $\pi^0$.

4a. It is generally believed that there are no asymmetries between quarks and antiquarks, and this belief has sparked many investigations toward understanding today's "baryon asymmetry," the complete dominance of matter over antimatter in our universe [29][30][31][32]. On the other hand, results from the LHCb experiment [33] indicated a substantial asymmetry (CP violation) in the weak decay of $\Lambda_b^0 \rightarrow p^+ \pi^- \pi^+ \pi^-$ (last reaction in Table 5 with $D^0 \rightarrow \pi^- \pi^+$ in the final state; see also [34] for similar LHCb results in weak decays of the charmed $D^0$ meson).

4b. In the course of this investigation, we uncovered a theoretical basis for CP violation in mesons. In Appendix C, we show that the energy levels of quarks and antiquarks are not symmetric, as is widely presumed. The energy cost for building higher-mass quarks is much less than for antiquarks, and their ground states also differ. In particular, building an $\bar{s}$ antiquark from its ground state (i.e., $\bar{d} \rightarrow \bar{s}$) costs 182 more MeV than building an s quark, i.e., $u \rightarrow s$ (Figure C1). These characteristic energy costs of (anti)quark transitions may be unobservable for now, but we hope they could at least be measured in lattice-QCD numerical simulations [35][36][37][38][39][40].

| Particle Symbol | Quark Content | Rest-mass $M$ (MeV) | $Q$ ($e$) | $I$ | $S$ | $C$ | $B'$ | $I_3$ | $Y$ | $Q'$ | $BF$ | $MD$ (MeV) |
|---|---|---|---|---|---|---|---|---|---|---|---|---|
| $p^+$ | uud | 938.27208 | +1 | 1/2 | 0 | 0 | 0 | 1/2 | 1 | 0 | 69.8 | 929.2821 |
| $n^0$ | udd | 939.56541 | 0 | 1/2 | 0 | 0 | 0 | −1/2 | 1 | 1 | 67.9 | 928.0654 |
| $\Lambda^0$ | uds | 1115.683 | 0 | 0 | −1 | 0 | 0 | 0 | 0 | 0 | 9.92 | 1015.45 |
| $\Sigma^0$ | uds | 1192.642 | 0 | 1 | −1 | 0 | 0 | 0 | 0 | 0 | 10.7 | 1092.41 |
| $\Sigma^+$ | uus | 1189.37 | +1 | 1 | −1 | 0 | 0 | 1 | 0 | −1 | 10.7 | 1091.65 |
| $\Sigma^-$ | dds | 1197.449 | −1 | 1 | −1 | 0 | 0 | −1 | 0 | 1 | 10.7 | 1094.71 |
| $\Xi^0$ | uss | 1314.86 | 0 | 1/2 | −2 | 0 | 0 | 1/2 | −1 | −1 | 5.89 | 1125.90 |
| $\Xi^-$ | dss | 1321.71 | −1 | 1/2 | −2 | 0 | 0 | −1/2 | −1 | 0 | 5.90 | 1130.24 |
| $\Lambda_c^+$ | udc | 2286.46 | +1 | 0 | 0 | 1 | 0 | 0 | 2 | 1 | 0.396 | 1009.6 |
| $\Lambda_b^0$ | udb | 5619.6 | 0 | 0 | 0 | 0 | −1 | 0 | 0 | 0 | 0.342 | 1432.8 |
| $\Sigma_c^{++}$ | uuc | 2453.97 | +2 | 1 | 0 | 1 | 0 | 1 | 2 | 0 | 0.463 | 1179.6 |
| $\Sigma_c^+$ | udc | 2452.9 | +1 | 1 | 0 | 1 | 0 | 0 | 2 | 1 | 0.461 | 1176.1 |
| $\Sigma_c^0$ | ddc | 2453.75 | 0 | 1 | 0 | 1 | 0 | −1 | 2 | 2 | 0.461 | 1174.4 |
| $\Xi_c'^+$ | usc | 2578.4 | +1 | 1/2 | −1 | 1 | 0 | 1/2 | 1 | 0 | 0.460 | 1212.8 |
| $\Xi_c'^0$ | dsc | 2579.2 | 0 | 1/2 | −1 | 1 | 0 | −1/2 | 1 | 1 | 0.459 | 1211.1 |
| $\Omega_c^0$ | ssc | 2695.2 | 0 | 0 | −2 | 1 | 0 | 0 | 0 | 0 | 0.454 | 1238.4 |
| $\Sigma_b^+$ | uub | 5810.56 | +1 | 1 | 0 | 0 | −1 | 1 | 0 | −1 | 0.388 | 1626.2 |
| $\Sigma_b^0$ | udb | (5810.56) | 0 | 1 | 0 | 0 | −1 | 0 | 0 | 0 | 0.388 | 1623.7 |
| $\Sigma_b^-$ | ddb | 5815.64 | −1 | 1 | 0 | 0 | −1 | −1 | 0 | 1 | 0.388 | 1626.3 |
| $\Omega_b^-$ | ssb | 6046.1 | −1 | 0 | −2 | 0 | −1 | 0 | −2 | −1 | 0.385 | 1679.3 |
| $\Xi_c^+$ | usc | 2467.94 | +1 | 1/2 | −1 | 1 | 0 | 1/2 | 1 | 0 | 0.418 | 1102.4 |
| $\Xi_c^0$ | dsc | 2470.90 | 0 | 1/2 | −1 | 1 | 0 | −1/2 | 1 | 1 | 0.418 | 1102.8 |
| $\Xi_{cc}^{++}$ | ucc | 3621.2 | +2 | 1/2 | 0 | 2 | 0 | 1/2 | 3 | 1 | 0.212 | 1079.0 |
| $\Xi_{cc}^+$ | dcc | (3621.2) | +1 | 1/2 | 0 | 2 | 0 | −1/2 | 3 | 2 | 0.212 | 1076.5 |
| $\Xi_b^0$ | usb | 5791.9 | 0 | 1/2 | −1 | 0 | −1 | 1/2 | −1 | −1 | 0.354 | 1516.3 |
| $\Xi_b^-$ | dsb | 5797.0 | −1 | 1/2 | −1 | 0 | −1 | −1/2 | −1 | 0 | 0.355 | 1518.9 |
| $\Xi_b'^0$ | usb | (5791.9) | 0 | 1/2 | −1 | 0 | −1 | 1/2 | −1 | −1 | 0.354 | 1516.3 |
| $\Xi_b'^-$ | dsb | (5797.0) | −1 | 1/2 | −1 | 0 | −1 | −1/2 | −1 | 0 | 0.355 | 1518.9 |

**Table 1.** The $J^{\mathrm{P}} = (1/2)^+$ baryon octet followed by additional high-mass $J^{\mathrm{P}} = (1/2)^+$ baryon states.


doi.org/10.32388/ZM7QNO

| Particle Symbol | Quark Content | Rest-mass $M$ (MeV) | $Q$ ($e$) | $I$ | $S$ | $C$ | $B'$ | $I_3$ | $Y$ | $Q'$ | $BF$ | $MD$ (MeV) |
|---|---|---|---|---|---|---|---|---|---|---|---|---|
| $\Delta^{++}$ | uuu | 1232 | $+2$ | $3/2$ | 0 | 0 | 0 | $3/2$ | 1 | $-1$ | 94.6 | 1225.5 |
| $\Delta^{+}$ | uud | 1232 | $+1$ | $3/2$ | 0 | 0 | 0 | $1/2$ | 1 | 0 | 91.9 | 1223.0 |
| $\Delta^{0}$ | udd | 1232 | 0 | $3/2$ | 0 | 0 | 0 | $-1/2$ | 1 | 1 | 89.3 | 1220.5 |
| $\Delta^{-}$ | ddd | 1232 | $-1$ | $3/2$ | 0 | 0 | 0 | $-3/2$ | 1 | 2 | 86.9 | 1218.0 |
| $\Sigma^{*+}$ | uus | 1382.80 | $+1$ | 1 | $-1$ | 0 | 0 | 1 | 0 | $-1$ | 12.6 | 1285.1 |
| $\Sigma^{*0}$ | uds | 1383.7 | 0 | 1 | $-1$ | 0 | 0 | 0 | 0 | 0 | 12.5 | 1283.5 |
| $\Sigma^{*-}$ | dds | 1387.2 | $-1$ | 1 | $-1$ | 0 | 0 | $-1$ | 0 | 1 | 12.5 | 1284.5 |
| $\Xi^{*0}$ | uss | 1531.80 | 0 | $1/2$ | $-2$ | 0 | 0 | $1/2$ | $-1$ | $-1$ | 7.03 | 1342.8 |
| $\Xi^{*-}$ | dss | 1535.0 | $-1$ | $1/2$ | $-2$ | 0 | 0 | $-1/2$ | $-1$ | 0 | 7.02 | 1343.5 |
| $\Omega^{-}$ | sss | 1672.45 | $-1$ | 0 | $-3$ | 0 | 0 | 0 | $-2$ | $-1$ | 4.97 | 1392.3 |
| $\Sigma_c^{*++}$ | uuc | 2518.41 | $+2$ | 1 | 0 | 1 | 0 | 1 | 2 | 0 | 0.488 | 1244.1 |
| $\Sigma_c^{*+}$ | udc | 2517.5 | $+1$ | 1 | 0 | 1 | 0 | 0 | 2 | 1 | 0.487 | 1240.7 |
| $\Sigma_c^{*0}$ | ddc | 2518.48 | 0 | 1 | 0 | 1 | 0 | $-1$ | 2 | 2 | 0.486 | 1239.1 |
| $\Xi_c^{*+}$ | usc | 2645.56 | $+1$ | $1/2$ | $-1$ | 1 | 0 | $1/2$ | 1 | 0 | 0.485 | 1280.0 |
| $\Xi_c^{*0}$ | dsc | 2646.38 | 0 | $1/2$ | $-1$ | 1 | 0 | $-1/2$ | 1 | 1 | 0.485 | 1278.3 |
| $\Omega_c^{*0}$ | ssc | 2765.9 | 0 | 0 | $-2$ | 1 | 0 | 0 | 0 | 0 | 0.480 | 1309.1 |
| $\Sigma_b^{*+}$ | uub | 5830.32 | $+1$ | 1 | 0 | 0 | $-1$ | 1 | 0 | $-1$ | 0.393 | 1646.0 |
| $\Sigma_b^{*0}$ | udb | (5830.32) | 0 | 1 | 0 | 0 | $-1$ | 0 | 0 | 0 | 0.392 | 1643.5 |
| $\Sigma_b^{*-}$ | ddb | 5834.74 | $-1$ | 1 | 0 | 0 | $-1$ | $-1$ | 0 | 1 | 0.393 | 1645.4 |
| $\Xi_b^{*0}$ | usb | 5952.3 | 0 | $1/2$ | $-1$ | 0 | $-1$ | $1/2$ | $-1$ | $-1$ | 0.392 | 1676.7 |
| $\Xi_b^{*-}$ | dsb | 5955.33 | $-1$ | $1/2$ | $-1$ | 0 | $-1$ | $-1/2$ | $-1$ | 0 | 0.392 | 1677.3 |

**Table 2.** The $J^{\mathrm{P}} = (3/2)^{+}$ baryon decuplet followed by additional $J^{\mathrm{P}} = (3/2)^{+}$ baryon states.

| Particle Symbol | Quark Content | Rest-mass $M$ (MeV) | $Q$ ($e$) | $I$ | $S$ | $C$ | $B'$ | $I_3$ | $Y$ | $Q'$ | $BF$ | $MD$ (MeV) |
|---|---|---|---|---|---|---|---|---|---|---|---|---|
| $\pi^+$ | $u\bar{d}$ | 139.5704 | +1 | 1 | 0 | 0 | 0 | 1 | 0 | −1 | 14.8 | 132.74 |
| $\pi^-$ | $d\bar{u}$ | 139.5704 | −1 | 1 | 0 | 0 | 0 | −1 | 0 | 1 | 14.8 | 132.74 |
| $\pi^0$ | $\frac{u\bar{u}-d\bar{d}}{\sqrt{2}}$ | 134.9768 | 0 | 1 | 0 | 0 | 0 | 0 | 0 | 0 | 14.3 | 128.15 |
| $\eta$ | $\frac{u\bar{u}+d\bar{d}-2s\bar{s}}{\sqrt{6}}$ | 547.862 | 0 | 0 | 0 | 0 | 0 | 0 | 0 | 0 | ⋯ | ⋯ |
| $\eta'$ | $\frac{u\bar{u}+d\bar{d}+s\bar{s}}{\sqrt{3}}$ | 957.78 | 0 | 0 | 0 | 0 | 0 | 0 | 0 | 0 | ⋯ | ⋯ |
| $K^+$ | $u\bar{s}$ | 493.677 | +1 | 1/2 | 1 | 0 | 0 | 1/2 | 1 | 0 | 4.07 | 398.12 |
| $K^-$ | $s\bar{u}$ | 493.677 | −1 | 1/2 | −1 | 0 | 0 | −1/2 | −1 | 0 | 4.07 | 398.12 |
| $K^0$ | $d\bar{s}$ | 497.611 | 0 | 1/2 | 1 | 0 | 0 | −1/2 | 1 | 1 | 4.07 | 399.54 |
| $\bar{K}^0$ | $s\bar{d}$ | 497.611 | 0 | 1/2 | −1 | 0 | 0 | 1/2 | −1 | −1 | 4.07 | 399.54 |
| HIGH-MASS $\eta$-MESONS ($J^P = 0^-$) | | | | | | | | | | | | |
| $\eta_c(1s)$ | $c\bar{c}$ | 2983.9 | 0 | 0 | 0 | 0 | 0 | 0 | 0 | 0 | 0.0874 | 443.9 |
| $\eta_b(1s)$ | $b\bar{b}$ | 9398.7 | 0 | 0 | 0 | 0 | 0 | 0 | 0 | 0 | 0.124 | 1038.7 |
| D-MESONS ($J^P = 0^-$) | | | | | | | | | | | | |
| $D^+$ | $c\bar{d}$ | 1869.61 | +1 | 1/2 | 0 | 1 | 0 | 1/2 | 1 | 0 | 0.234 | 594.9 |
| $D^0$ | $c\bar{u}$ | 1864.84 | 0 | 1/2 | 0 | 1 | 0 | −1/2 | 1 | 1 | 0.233 | 592.7 |
| $D_s^+$ | $c\bar{s}$ | 1968.30 | +1 | 0 | 1 | 1 | 0 | 0 | 2 | 1 | 0.230 | 604.9 |
| $D_s^-$ | $s\bar{c}$ | 1968.30 | −1 | 0 | −1 | −1 | 0 | 0 | −2 | −1 | 0.230 | 604.9 |
| B-MESONS ($J^P = 0^-$) | | | | | | | | | | | | |
| $B^+$ | $u\bar{b}$ | 5279.34 | +1 | 1/2 | 0 | 0 | 1 | 1/2 | 1 | 0 | 0.262 | 1097.2 |
| $B^0$ | $d\bar{b}$ | 5279.65 | 0 | 1/2 | 0 | 0 | 1 | −1/2 | 1 | 1 | 0.262 | 1095.0 |
| $B_s^0$ | $s\bar{b}$ | 5366.88 | 0 | 0 | −1 | 0 | 1 | 0 | 0 | 0 | 0.256 | 1093.5 |
| $B_c^+$ | $c\bar{b}$ | 6274.9 | +1 | 0 | 0 | 1 | 1 | 0 | 2 | 1 | 0.123 | 824.9 |
| VECTOR MESONS ($J^P = 1^-$) | | | | | | | | | | | | |
| $\rho^+$ | $u\bar{d}$ | 775.11 | +1 | 1 | 0 | 0 | 0 | 1 | 0 | −1 | 85.5 | 768.28 |
| $\rho^-$ | $d\bar{u}$ | 775.11 | −1 | 1 | 0 | 0 | 0 | −1 | 0 | 1 | 85.5 | 768.28 |
| $\rho^0$ | $\frac{u\bar{u}-d\bar{d}}{\sqrt{2}}$ | 775.26 | 0 | 1 | 0 | 0 | 0 | 0 | 0 | 0 | 85.6 | 768.43 |
| $\omega$ | $\frac{u\bar{u}+d\bar{d}}{\sqrt{2}}$ | 782.66 | 0 | 0 | 0 | 0 | 0 | 0 | 0 | 0 | 86.4 | 775.83 |
| $K^{*+}$ | $u\bar{s}$ | 891.66 | +1 | 1/2 | 1 | 0 | 0 | 1/2 | 1 | 0 | 8.15 | 796.10 |
| $K^{*0}$ | $d\bar{s}$ | 895.81 | 0 | 1/2 | 1 | 0 | 0 | −1/2 | 1 | 1 | 8.13 | 797.74 |
| $\phi$ | $s\bar{s}$ | 1019.461 | 0 | 0 | 0 | 0 | 0 | 0 | 0 | 0 | 4.46 | 832.7 |
| J/ψ $(1s)$ | $c\bar{c}$ | 3096.916 | 0 | 0 | 0 | 0 | 0 | 0 | 0 | 0 | 0.110 | 556.9 |
| Υ $(1s)$ | $b\bar{b}$ | 9460.30 | 0 | 0 | 0 | 0 | 0 | 0 | 0 | 0 | 0.132 | 1100.3 |
| $D^{*+}$ | $c\bar{d}$ | 2010.26 | +1 | 1/2 | 0 | 1 | 0 | 1/2 | 1 | 0 | 0.289 | 735.6 |
| $D^{*0}$ | $c\bar{u}$ | 2006.96 | 0 | 1/2 | 0 | 1 | 0 | −1/2 | 1 | 1 | 0.289 | 734.8 |
| $D_s^{*+}$ | $c\bar{s}$ | 2112.1 | +1 | 0 | 1 | 1 | 0 | 0 | 2 | 1 | 0.284 | 748.7 |
| $B^{*+}$ | $u\bar{b}$ | 5325.2 | +1 | 1/2 | 0 | 0 | 1 | 1/2 | 1 | 0 | 0.273 | 1143.0 |
| $B^{*0}$ | $d\bar{b}$ | 5325.2 | 0 | 1/2 | 0 | 0 | 1 | −1/2 | 1 | 1 | 0.273 | 1140.5 |
| $B_s^{*0}$ | $s\bar{b}$ | 5415.4 | 0 | 0 | −1 | 0 | 1 | 0 | 0 | 0 | 0.267 | 1142.0 |
| $B_c^{*+}$ | $c\bar{b}$ | (6274.9) | +1 | 0 | 0 | 1 | 1 | 0 | 2 | 1 | 0.123 | 824.9 |

**Table 3.** The $J^P = 0^-$ pseudoscalar meson nonet followed by additional meson states (the $J^P = 0^-$ high-

mass $\eta$-mesons, D-mesons, and B-mesons; and the $J^{\mathrm{P}} = 1^{-}$ vector mesons).

| | u | d | s | c | b | t |
|---|---|---|---|---|---|---|
| Rest-masses | | | | | | |
| | 2.16 MeV | 4.67 MeV | 93.4 MeV | 1.27 GeV | 4.18 GeV | 172.5 GeV |
| Quantum Numbers | | | | | | |
| All Interactions | | | | | | |
| $Q$ | $2/3$ | $-1/3$ | $-1/3$ | $2/3$ | $-1/3$ | $2/3$ |
| Strong Interactions | | | | | | |
| $I_3$ | $1/2$ | $-1/2$ | $0$ | $0$ | $0$ | $0$ |
| $Y$ | $1/3$ | $1/3$ | $-2/3$ | $4/3$ | $-2/3$ | $4/3$ |
| $Q'$ [a] | $-1/3$ | $2/3$ | $-1/3$ | $2/3$ | $-1/3$ | $2/3$ |
| Weak Interactions | | | | | | |
| $I_{3\mathrm{w}}$ | $1/2$ | $-1/2$ | $-1/2$ | $1/2$ | $-1/2$ | $1/2$ |
| $Y_{\mathrm{w}}$ | $1/3$ | $1/3$ | $1/3$ | $1/3$ | $1/3$ | $1/3$ |
| $Q'_{\mathrm{w}}$ [b] | $-1/3$ | $2/3$ | $2/3$ | $-1/3$ | $2/3$ | $-1/3$ |

**Table 4.** Rest-masses and quantum numbers of quarks.

[a] No other quantum number, strong or weak, exhibits the u-d/s-c/b-t ($-1/3, +2/3$) symmetry seen in the strong charge $Q' = Y - Q$ in each generation with increasing mass.

[b] Weak charge $Q'_{\mathrm{w}} \equiv Y_{\mathrm{w}}/2 - I_{3\mathrm{w}} = Y_{\mathrm{w}} - Q$; it does not exhibit the same symmetry as its strong counterpart $Q'$---a fundamental distinction between the strong and the weak charge, although the EM charge $Q$ couples to both of these charges in the same fashion.


doi.org/10.32388/ZM7QNO

| Decay | $Q'$ | $ML$ (s) |
|---|---|---|
| The only strong/EM decay in the octet is | | |
| $\Sigma^0 \to \Lambda^0 \gamma_{(77\,\mathrm{MeV})}$ | $0 \to 0\,0 = 0$ | $7.4 \times 10^{-20}$ |
| All other octet decays go to pions/leptons and are weak, e.g., | | |
| $n^0 \to p^+ e^- \overline{\nu}_e$ | $1 \to 0\,0\,0 = 0$ | 878.4 |
| $\Sigma^+ \to p^+ \pi^0$ | -1 $\to 0\,0 = 0$ | $8.0 \times 10^{-11}$ |
| $\Xi^- \to \Lambda^0 \pi^-$ | $0 \to 0\,1 = 1$ | $1.6 \times 10^{-10}$ |
| NOTES: | | |
| Higher-energy states do show strong/EM decays, e.g., | | |
| $\Sigma_c^0 \to \Lambda_c^+ \pi^-$ | $2 \to 1\,1 = 2$ | $3.6 \times 10^{-22}$ |
| $\Omega_b^- \to \Omega^- \mathrm{J/\psi}$ | -1$\to$ -1 0 = -1 | $1.6 \times 10^{-12}$ |
| $\Lambda_b^0 \to \Lambda_c^+ \mathrm{D_s^-}$ | $0 \to 1$ -1 $= 0$ | $1.5 \times 10^{-12}$ |
| but $\Lambda_c^+$ and $\Omega_c^0$ are noted for not having strong/EM decays | | |
| $\Lambda_c^+ \to \Lambda^0 \pi^+ \eta$ | $1 \to 0$ -1 0 = -1 | $2.0 \times 10^{-13}$ |
| $\Omega_c^0 \to \Xi^0 \mathrm{K^-} \pi^+$ | 0$\to$ -1 0 -1 = -2 | $2.7 \times 10^{-13}$ |
| and $\Lambda_b^0$ is noted for having also some weak decays, e.g., | | |
| $\Lambda_b^0 \to p^+ \mathrm{D^0} \pi^-$ | $0 \to 0\,1\,1 = 2$ | $1.5 \times 10^{-12}$ |
| or with a $\mathrm{K^-}$ been emitted in place of $\pi^-$ (then $Q' = 0 \to 1$). | | |

**Table 5.** Strong/EM $J^{\mathrm{P}} = (1/2)^+$ baryon modes (referring to the octet listed at the top of Table 1) and mean lifetimes ($ML$) in seconds.

| Decay | $Q'$ | $ML$ (s) |
|---|---|---|
| All decuplet decays are strong/EM, e.g., | | |
| $\Delta^{++} \to p^+ \pi^+$ | 1→ 0 1 = 1 | $5.6 \times 10^{-24}$ |
| $\Delta^- \to n^0 \pi^-$ | 2→ 1 1 = 2 | $5.6 \times 10^{-24}$ |
| $\Sigma^{*-} \to \Lambda^0 \pi^-$ | 1→ 0 1 = 1 | $1.7 \times 10^{-23}$ |
| $\Xi^{*0} \to \Xi^- \pi^+$ | 1→ 0 1 = 1 | $7.2 \times 10^{-23}$ |
| $\Xi^{*0} \to \Xi^0 \pi^0$ | 1→ 1 0 = 1 | $7.2 \times 10^{-23}$ |
| except for $\Omega^-$ (which is then quite long-lived), e.g., | | |
| $\Omega^- \to \Lambda^0 \mathrm{K}^-$ | 1→ 0 0 = 0 | $8.2 \times 10^{-11}$ |
| NOTES: | | |
| All higher-energy states also show strong/EM decays, e.g., | | |
| $\Sigma_c^{*0} \to \Lambda_c^+ \pi^-$ | 2 → 1 1 = 2 | $4.3 \times 10^{-23}$ |
| $\Sigma_b^{*+} \to \Lambda_b^0 \pi^+$ | 1 → 0 1 = 1 | $7.0 \times 10^{-23}$ |
| $\Xi_c^{*0} \to \Xi_c^+ \pi^-$ | 1 → 0 1 = 1 | $2.8 \times 10^{-22}$ |
| $\Xi_b^{*0} \to \Xi_b^- \pi^+$ | 1 → 0 1 = 1 | $7.3 \times 10^{-22}$ |
| $\Omega_c^{*0} \to \Omega_c^0 \gamma_{(70.7\,\mathrm{MeV})}$ | 0 → 0 0 = 0 | Unknown |

**Table 6.** Strong/EM $J^{\mathrm{P}} = (3/2)^+$ baryon modes (referring to the decuplet listed at the top of Table 2) and mean lifetimes ($ML$) in seconds.

| Decay | $Q'$ | $ML$ (s) |
|---|---|---|
| Some pion decays and the $\eta, \eta'$ decays are strong/EM, e.g., | | |
| $\pi^0 \to (2\gamma)_{(135\,\mathrm{MeV})}$ | $0 \to 0\,0 = 0$ | $8.5 \times 10^{-17}$ |
| $\eta \to \pi^+\,\pi^0\,\pi^-$ | $0 \to$ -1 0 1 $= 0$ | $5.0 \times 10^{-19}$ |
| $\eta' \to \pi^+\,\pi^-\,\eta$ | $0 \to$ -1 1 0 $= 0$ | $3.3 \times 10^{-21}$ |
| $\eta' \to \rho^0\,\gamma_{(182.5\,\mathrm{MeV})}$ | $0 \to 0\,0 = 0$ | $3.3 \times 10^{-21}$ |
| Kaon decays are weak, e.g., | | |
| $\mathrm{K}^+ \to \mu^+\,\nu_\mu$ | $0 \to$ -1 0 $=$ -1 | $1.2 \times 10^{-8}$ |
| $\mathrm{K}^0_{(\mathrm{L})} \to 3\pi^0$ | $1 \to 0\,0\,0 = 0$ | $5.1 \times 10^{-8}$ |
| NOTES: Higher-energy states (D and B mesons) show but a few strong/EM decays, viz. | | |
| $\mathrm{D}^+ \to \mathrm{K}^0\,\pi^+$ | $0 \to 1$ -1 $= 0$ | $1.0 \times 10^{-12}$ |
| $\mathrm{B}^+ \to \mathrm{K}^0\,\pi^+$ | $0 \to 1$ -1 $= 0$ | $1.6 \times 10^{-12}$ |
| $\mathrm{B}^0_\mathrm{s} \to \mathrm{J}/\psi\,\pi^+\,\pi^-$ | $0 \to 0$ -1 1 $= 0$ | $1.5 \times 10^{-12}$ |
| $\mathrm{B}^+_\mathrm{c} \to \mathrm{D}^+_\mathrm{s}\,\phi$ | $1 \to 1\,0 = 1$ | $4.5 \times 10^{-13}$ |
| The famous production of $\Omega^-$ [24,25] is strong, viz. | | |
| $\mathrm{K}^-\,p^+ \to \Omega^-\,\mathrm{K}^+\,\mathrm{K}^0$ | $0\,0 \to$ -1 0 1 $= 0$ | |
| but subsequent decays are weak: $\mathrm{K}^0 \to \pi^+\,\pi^-$ ($Q' = 1 \to 0$) and $\Omega^- \to \Lambda^0\,\mathrm{K}^-$ ($Q' =$ -1$\to 0$). It is interesting that kaons are produced in strong decays, but then they decay only via the weak interaction. | | |

**Table 7.** Strong/EM $J^\mathrm{P} = 0^-$ pseudoscalar meson modes (referring to the nonet listed at the top of Table 3) and mean lifetimes ($ML$) in seconds.

| Decay | $Q'$ | $ML$ (s) |
|---|---|---|
| All nonet decays are strong/EM, e.g., | | |
| $\rho^+ \to \pi^+ \pi^0$ | $\text{-}1 \to \text{-}1\,0 = \text{-}1$ | $4.4 \times 10^{-24}$ |
| $\rho^- \to \pi^- \eta$ | $1 \to 1\,0 = 1$ | $4.4 \times 10^{-24}$ |
| $\rho^0 \to \pi^+ \pi^-$ | $0 \to \text{-}1\,1 = 0$ | $4.5 \times 10^{-24}$ |
| $\omega \to \pi^+ \pi^0 \pi^-$ | $0 \to \text{-}1\,0\,1 = 0$ | $7.8 \times 10^{-23}$ |
| $\phi \to \mathrm{K}^+ \mathrm{K}^-$ | $0 \to 0\,0 = 0$ | $1.5 \times 10^{-22}$ |
| $\mathrm{K}^{*+} \to \mathrm{K}^0 \pi^+$ | $0 \to 1\ \text{-}1 = 0$ | $3.3 \times 10^{-23}$ |
| $\mathrm{K}^{*0} \to \mathrm{K}^+ \pi^-$ | $1 \to 0\,1 = 1$ | $1.4 \times 10^{-23}$ |
| NOTES: | | |
| Higher-energy states ($\mathrm{D}^*$ and $\mathrm{B}^*$ mesons) show strong/EM decays in almost all cases, e.g., | | |
| $\mathrm{D}^{*+} \to \mathrm{D}^0 \pi^+$ | $0 \to 1\ \text{-}1 = 0$ | $7.9 \times 10^{-21}$ |
| $\mathrm{B}_\mathrm{s}^{*0} \to \mathrm{B}_\mathrm{s}^0 \gamma_{(48.6\,\mathrm{MeV})}$ | $0 \to 0\ 0 = 0$ | Unknown |
| except for a striking exception, the weak decay | | |
| $\mathrm{D}_\mathrm{s}^{*+} \to \mathrm{D}^{*+} \pi^0$ | $1 \to 0\ 0 = 0$ | $>3.4 \times 10^{-22}$ |
| or with a photon $\gamma_{(101.8\,\mathrm{MeV})}$ been emitted in place of $\pi^0$. | | |

**Table 8.** Strong/EM $J^\mathrm{P} = 1^-$ vector meson modes (referring to the ($\rho, \phi, \omega, \mathrm{K}^*$) nonet listed at the lower part of Table 3) and mean lifetimes ($ML$) in seconds.

| EM or ST? | Decay | $Q'$ | $\lvert Q-Q'\rvert$ | $ML$ (s) |
|---|---|---|---|---|
| | Case 1: $\lvert Q-Q'\rvert \equiv 0$ on the left side and across the entire decay reaction. The 8 such examples from Tables 5-8 are: | | | |
| | $\Sigma^0 \to \Lambda^0 \gamma$ | $0 \to 0\,0 = 0$ | $0 \to 0\,0 = 0$ | $7.4 \times 10^{-20}$ |
| | $\Omega_b^- \to \Omega^- J/\psi$ | -1$\to$ -1 0 = -1 | $0 \to 0\,0 = 0$ | $1.6 \times 10^{-12}$ |
| | $\Lambda_b^0 \to \Lambda_c^+ D_s^-$ | $0 \to 1$ -1 $= 0$ | $0 \to 0\,0 = 0$ | $1.5 \times 10^{-12}$ |
| | $\Omega_c^{*0} \to \Omega_c^0 \gamma$ | $0 \to 0\,0 = 0$ | $0 \to 0\,0 = 0$ | Unknown |
| | $\pi^0 \to \gamma\gamma$ | $0 \to 0\,0 = 0$ | $0 \to 0\,0 = 0$ | $8.5 \times 10^{-17}$ |
| | $\eta' \to \rho^0 \gamma$ | $0 \to 0\,0 = 0$ | $0 \to 0\,0 = 0$ | $3.3 \times 10^{-21}$ |
| | $B_c^+ \to D_s^+ \phi$ | $1 \to 1\,0 = 1$ | $0 \to 0\,0 = 0$ | $4.5 \times 10^{-13}$ |
| | $B_s^{*0} \to B_s^0 \gamma$ | $0 \to 0\,0 = 0$ | $0 \to 0\,0 = 0$ | Unknown |
| EM | When $\lvert Q-Q'\rvert \equiv 0$ across the decay reaction, then $I_3 \equiv 0$ and it does not appear in the wavefunctions. Isospin (non)conservation then becomes a meaningless distinction. Photon emission in many reactions also reveals their predominantly EM nature. Note: The *ML*s of $\Omega_b^-$, $\Lambda_b^0$, and $B_c^+$ are long, so weak interactions are involved too. | | | |
| | Case 2: $\lvert Q-Q'\rvert \neq 0$ on the left side, and conserved across the reaction. The 9 such examples from Tables 5-8 are: | | | |
| | $\Delta^{++} \to p^+ \pi^+$ | -1$\to$ 0 -1 = -1 | $3 \to 1\,2 = 3$ | $5.6 \times 10^{-24}$ |
| | $\Delta^- \to n^0 \pi^-$ | 2$\to$ 1 1 = 2 | $3 \to 1\,2 = 3$ | $5.6 \times 10^{-24}$ |
| | $\Sigma^{*-} \to \Lambda^0 \pi^-$ | 1$\to$ 0 1 = 1 | $2 \to 0\,2 = 2$ | $1.7 \times 10^{-23}$ |
| | $\Xi^{*0} \to \Xi^0 \pi^0$ | -1$\to$ -1 0 = -1 | $1 \to 1\,0 = 1$ | $7.2 \times 10^{-23}$ |
| | $\Sigma_c^0 \to \Lambda_c^+ \pi^-$ | $2 \to 1\,1 = 2$ | $2 \to 0\,2 = 2$ | $3.6 \times 10^{-22}$ |
| | $\Sigma_c^{*0} \to \Lambda_c^+ \pi^-$ | $2 \to 1\,1 = 2$ | $2 \to 0\,2 = 2$ | $4.3 \times 10^{-23}$ |
| | $\Sigma_b^{*+} \to \Lambda_b^0 \pi^+$ | -1 $\to$ 0 -1 = -1 | $2 \to 0\,2 = 2$ | $7.0 \times 10^{-23}$ |
| | $\rho^+ \to \pi^+ \pi^0$ | -1 $\to$ -1 0 = -1 | $2 \to 2\,0 = 2$ | $4.4 \times 10^{-24}$ |
| | $\rho^- \to \pi^- \eta$ | $1 \to 1\,0 = 1$ | $2 \to 2\,0 = 2$ | $4.4 \times 10^{-24}$ |
| ST | When $\lvert Q-Q'\rvert \neq 0$ and conserved in the decay, then $\lvert I_3\rvert$ is also conserved. Then, the decay reaction is mediated primarily by the strong interaction. Note: All *ML*s are very short, a typical property of predominantly strong decays. | | | |
| | Case 3: $\lvert Q-Q'\rvert \neq 0$ on at least one side, and not conserved across the reaction. The 14 such examples from Tables 6-8 are: | | | |
| | $\Xi^{*0} \to \Xi^- \pi^+$ | -1$\to$ 0 -1 = -1 | $1 \to 1\,2 = 3$ | $7.2 \times 10^{-23}$ |
| | $\Xi_c^{*0} \to \Xi_c^+ \pi^-$ | 1 $\to$ 0 1 = 1 | $1 \to 1\,2 = 3$ | $2.8 \times 10^{-22}$ |
| | $\Xi_b^{*0} \to \Xi_b^- \pi^+$ | -1 $\to$ 0 -1 = -1 | $1 \to 1\,2 = 3$ | $7.3 \times 10^{-22}$ |
| | $\eta \to \pi^+ \pi^0 \pi^-$ | 0 $\to$ -1 0 1 = 0 | $0 \to 2\,0\,2 = 4$ | $5.0 \times 10^{-19}$ |
| | $\eta' \to \pi^+ \pi^- \eta$ | 0 $\to$ -1 1 0 = 0 | $0 \to 2\,2\,0 = 4$ | $3.3 \times 10^{-21}$ |
| | $D^+ \to K^0 \pi^+$ | 0 $\to$ 1 -1 = 0 | $1 \to 1\,2 = 3$ | $1.0 \times 10^{-12}$ |
| | $B^+ \to K^0 \pi^+$ | 0 $\to$ 1 -1 = 0 | $1 \to 1\,2 = 3$ | $1.6 \times 10^{-12}$ |
| | $B_s^0 \to J/\psi \pi^+ \pi^-$ | 0 $\to$ 0 -1 1 = 0 | $0 \to 0\,2\,2 = 4$ | $1.5 \times 10^{-12}$ |
| | $\rho^0 \to \pi^+ \pi^-$ | 0 $\to$ -1 1 = 0 | $0 \to 2\,2 = 4$ | $4.5 \times 10^{-24}$ |
| | $\omega \to \pi^+ \pi^0 \pi^-$ | 0 $\to$ -1 0 1 = 0 | $0 \to 2\,0\,2 = 4$ | $7.8 \times 10^{-23}$ |
| | $\phi \to K^+ K^-$ | 0 $\to$ 0 0 = 0 | $0 \to 1\,1 = 2$ | $1.5 \times 10^{-22}$ |
| | $K^{*+} \to K^0 \pi^+$ | 0 $\to$ 1 -1 = 0 | $1 \to 1\,2 = 3$ | $3.3 \times 10^{-23}$ |
| | $K^{*0} \to K^+ \pi^-$ | 1 $\to$ 0 1 = 1 | $1 \to 1\,2 = 3$ | $1.4 \times 10^{-23}$ |
| | $D^{*+} \to D^0 \pi^+$ | 0 $\to$ 1 -1 = 0 | $1 \to 1\,2 = 3$ | $7.9 \times 10^{-21}$ |
| EM | When $\lvert Q-Q'\rvert \neq 0$ on at least one side and not conserved, then $\lvert I_3\rvert$ is not conserved either. Then, the decay reaction is mediated primarily by the EM interaction. Note: The *ML*s of $D^+$, $B^+$, and $B_s^0$ are long, so weak interactions are involved too. | | | |


doi.org/10.32388/ZM7QNO

**Table 9.** Classification of the 31 non-weak ($Q'$-conserving) decays from Tables 5-8 into strong (ST) or EM, based on the behavior of the charge distance $|Q - Q'|$; and corresponding mean lifetimes ($ML$) in seconds.

# Appendix

## *Appendix A. Mass jumps between particles*

Figures A1-A3 illustrate in some detail the jumps in rest-mass between individual particles. All jumps are noted in MeV. The corresponding average rest-mass energy levels are illustrated in Figures 4-6 in the main text, where discrete jumps are more clearly seen between states (or groups of related particles).

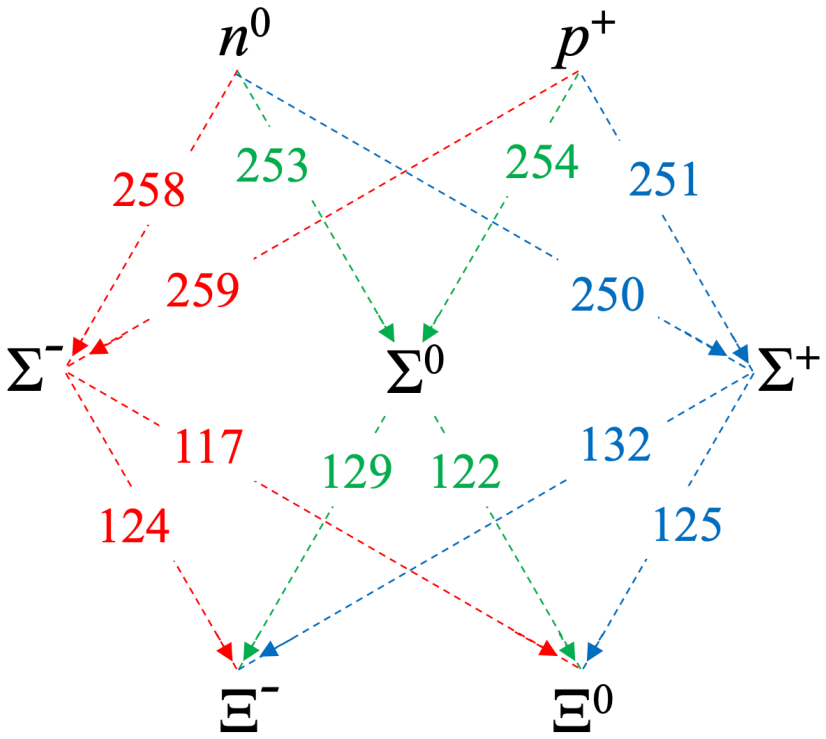


**Figure A1.** Detailed illustration of rest-mass energy levels for the $J^P = (1/2)^+$ baryons in Figure 4.


doi.org/10.32388/ZM7QNO

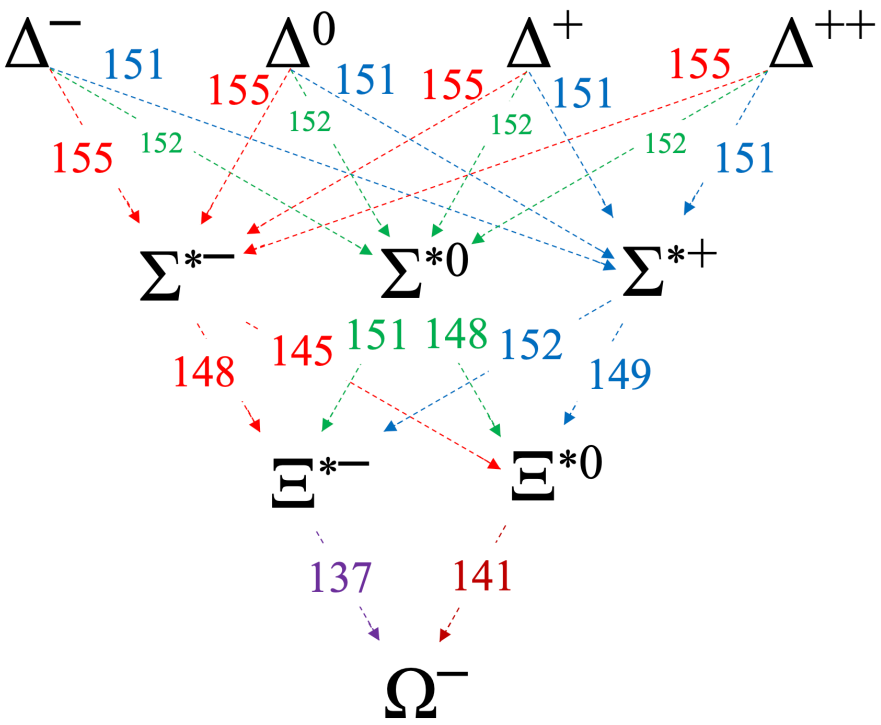


**Figure A2.** Detailed illustration of rest-mass energy levels for the $J^{\mathrm{P}} = (3/2)^{+}$ baryons in Figure 5.


doi.org/10.32388/ZM7QNO

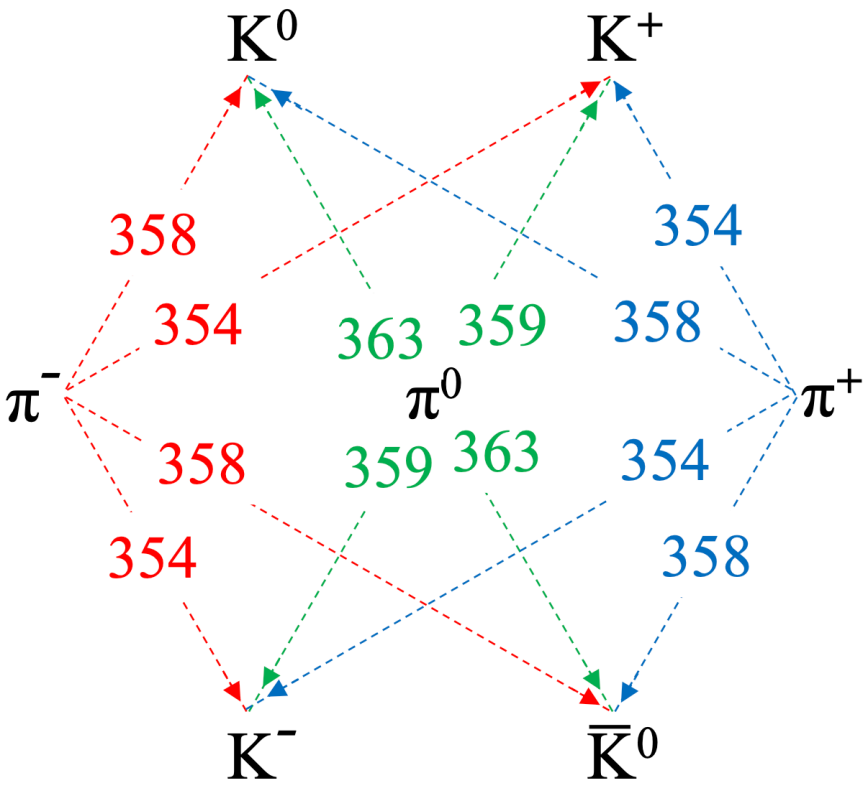


**Figure A3.** Detailed illustration of rest-mass energy levels for the low-mass $J^{\mathrm{P}} = 0^{-}$ pseudoscalar mesons in Figure 6.

## *Appendix B. Valence quarks in $\Sigma/\Lambda^0/\Xi/\Omega/\Xi^*$ baryons*

### *Appendix B1. Octet $\Sigma$ and $\Lambda^0$ baryons*

The $\Sigma^+$(uus) baryon is unusual in the sense that it is less massive than the neutral $\Sigma^0$(uds), whereas $\Sigma^-$(dds) is the most massive particle in the $\Sigma$-triplet (Table 1). It appears that the two low-mass u quarks in $\Sigma^+$ are responsible for this unusual outcome that persists in the *MD*s after we also account for the repulsive Coulomb content of the $\Sigma^{\pm}$ particles. ($\Sigma^+$ has the same charge layout as the proton, thus its strong field includes 1.22 MeV in suppressing the repulsion; similarly, the strong field of $\Sigma^-$ includes a Coulombic part of 1.00 MeV, as was found in § 3.3.) By subtracting the Coulombic contributions from the *MD*s of $\Sigma^{\pm}$ (Table 1), we obtain the remainders of the constituent energies $ER'$ of the $\Sigma$ excitations, viz.

$$\left.\begin{array}{l} \Sigma^+\,(\mathrm{uus}) \;:\; ER'_{\Sigma^+} = 1090.43 \\ \Sigma^0\;(\mathrm{uds}) \;:\; ER'_{\Sigma^0} = 1092.41 \\ \Sigma^-\,(\mathrm{dds}) \;:\; ER'_{\Sigma^-} = 1093.71 \end{array}\right\} \mathrm{MeV}. \tag{B.1}$$


doi.org/10.32388/ZM7QNO

Dynamic field support for two u quarks and one s quark is included in $ER'_{\Sigma^+}$ which is the lowest value. The other two higher values describe support for one and two d quarks relative to one and two u quarks, respectively, in $ER'_{\Sigma^+}$. But there is a caveat in the case of $\Sigma^0$ that differentiates it from the charged members of the triplet, despite all members having isospin $I = 1$: $\Sigma^0$ is an excitation of $\Lambda^0$ which has $I = 0$, as opposed to $\Sigma^{\pm}$ that are nucleonic ($I = 1/2$) excitations with isospin transitions of the form $I = 1/2 \to 1$. The cost in supporting the $I = 0 \to 1$ transition of $\Lambda^0 \to \Sigma^0$ can be obtained from the decay $\Sigma^0 \to \Lambda^0\,\gamma$ in which the emitted photon carries 76.959 MeV. Thus, the $I = 0 \to 1$ cost in isospin energy ($EI$), rounded to two decimals, is

$$EI_{0\to 1} = 76.96\ \mathrm{MeV}. \tag{B.2}$$

We note that hypercharge $Y$ does not capture the above difference, as it changes uniformly ($Y = 1 \to 0$) in nucleonic $\Lambda$ and $\Sigma$ excitations (Table 1).

We consider next transitions from the nucleonic ground state. We subtract the reference $MD_{\mathrm{n}}$ value of $n^0$ from the $ER'$ values listed in equation (B.1), and we find the building blocks of energy $ER$ in the strong-field support of the $\Sigma^{\pm}$ and $\Lambda^0$ excitations, viz.

$$\left.\begin{array}{lll} n^0 \to \Sigma^+\ (\mathrm{dd} \to \mathrm{us}) & : & ER_{\Sigma^+} = 162.36 \\ n^0 \to \Sigma^-\ (\mathrm{u} \to \mathrm{s}) & : & ER_{\Sigma^-} = 165.64 \\ n^0 \to \Lambda^0\ (\mathrm{d} \to \mathrm{s}) & : & ER_{\Lambda^0} = 87.38 \end{array}\right\} \mathrm{MeV}. \tag{B.3}$$

These energy values include the energy to maintain the newborn quarks (e.g., us in $\Sigma^+$ relative to dd in $n^0$), and the energy costs for the limpid changes in isospin energy between states ($EI_{1/2\to 1}$ for $\Sigma^{\pm}$ and $EI_{1/2\to 0}$ for $\Lambda^0$).

The above energy costs introduce more unknowns to the problem than the experimental data can handle. Then, it is common practice in physics to adopt a physical model capable of resolving the indeterminacy. In what follows, we incorporate several additional (yet reasonable) assumptions concerning various energy differences between states:

1. The energy cost to maintain a quark flip becomes gain when the quarks flip in the opposite direction; that is, the energies of the u→d and d→u quark flips obey $E_{\mathrm{u}\to\mathrm{d}} = -E_{\mathrm{d}\to\mathrm{u}}$, and so on for all the other flips. Thus, quark flipping is assumed to be a reversible process.
2. The same property as in item (1) also holds for isospin energies, viz. $EI_{1/2\to 0} = -EI_{0\to 1/2}$ and $EI_{1/2\to 1} = -EI_{1\to 1/2}$. Thus, isospin transition is assumed to be a reversible process as well.
3. The energy cost to maintain a u→s quark flip is the sum of the costs u→d and d→s; that is, the energies obey $E_{\mathrm{u}\to\mathrm{s}} = E_{\mathrm{u}\to\mathrm{d}} + E_{\mathrm{d}\to\mathrm{s}}$, and so on for all the other striding quark flips.

4. The same property as in item (3) also holds for isospin energies, viz. $EI_{0\to 1} = EI_{0\to 1/2} + EI_{1/2\to 1}$.

Based on the above considerations, we use the values listed in equation (B.3) to set up a $3\times 4$ system of equations describing the breakdown of the various excitation energies relative to the $n^0$ nucleonic ground state, viz.

$$\left.\begin{array}{rcr} -E_{\mathrm{u}\to\mathrm{d}} + E_{\mathrm{d}\to\mathrm{s}} + EI_{1/2\to 1} &=& 162.36 \\ E_{\mathrm{u}\to\mathrm{d}} + E_{\mathrm{d}\to\mathrm{s}} + EI_{1/2\to 1} &=& 165.64 \\ E_{\mathrm{d}\to\mathrm{s}} - EI_{0\to 1/2} &=& 87.38 \end{array}\right\} \mathrm{MeV}. \tag{B.4}$$

The solution of this system specifies a unique value of

$$E_{\mathrm{u}\to\mathrm{d}} = 1.64\mathrm{MeV}, \tag{B.5}$$

and the reduced $2\times 3$ system

$$\left.\begin{array}{rcr} EI_{1/2\to 1} + E_{\mathrm{d}\to\mathrm{s}} &=& 164.00 \\ EI_{1/2\to 1} + EI_{0\to 1/2} &=& 76.62 \end{array}\right\} \mathrm{MeV}. \tag{B.6}$$

The latter equation appears to justify assumption (4) above; it implies that $EI_{0\to 1} = 76.62$ MeV, which is barely 0.44% lower than the precise experimental value quoted in equation ( B.2) above.

Yet, we do not believe that this small discrepancy of 0.34 MeV is due to the many approximations and assumptions incorporated in our calculations; and it is certainly not due to the many experimental values that we have used above. Instead, we think that the 0.34 MeV difference indicates a missing energy term, $EI_0$, that represents the initial cost of switching states from $I=0$ to $I=0+\varepsilon$, $\varepsilon\to 0$ (i.e., the energy associated with the birth of the isospin property in strong interactions).

If we further assume that

$$EI_{0+\varepsilon\to 1/2} = EI_{1/2\to 1}\ ,$$

in actual $I\neq 0$ isospin transitions, we obtain a complete solution and a clear picture of light-quark transitions in low-energy octet baryons, viz.

$$\left.\begin{array}{rcr} E_{\mathrm{u}\to\mathrm{d}} &=& 1.64 \\ E_{\mathrm{d}\to\mathrm{s}} &=& 125.69 \\ E_{\mathrm{u}\to\mathrm{s}} &=& 127.33 \\ EI_{\delta I=+\frac{1}{2}} &=& 38.31 \\ EI_{\delta I=+1} &=& 76.62 \\ EI_0 &=& 0.34 \end{array}\right\} \mathrm{MeV}, \tag{B.7}$$

where $EI_{\delta I}>0$ is the associated energy cost during transitions between states (obeying the property that $EI_{-\delta I} = -EI_{\delta I}$); and $EI_0 > 0$ is the energy cost to jump-start a transition from an initial $I=0$ state, viz.

$$EI_0 + EI_{\delta I=+1} = 76.96\text{MeV} \equiv EI_{0\to 1}\,, \tag{B.8}$$

as in the fundamental experimental result described by equation (B.2) above. Furthermore,

$$EI_0 + EI_{\delta I=+1/2} = 38.65\text{MeV} \equiv EI_{0\to 1/2}\,, \tag{B.9}$$

for the complete half-way process $EI_{0\to 1/2}$ with isospin change $I \equiv 0 \to 1/2$.

## *Appendix B.2. Discussion of the $\Sigma$-$\Lambda^0$ Results*

There is a wealth of information in the above results. Here we highlight a few key points:

a. The u→d quark flip is inexpensive ($E_{\text{u}\to\text{d}} = 1.64$ MeV). This explains why u→d is the only flip to a higher-mass quark in the quark sequence [24]. The transition involves the exchange of a virtual $W^-$ boson of mass 80.377 GeV [2], so the actual flipping cost $E_{\text{u}\to\text{d}}$ is truly negligible. Furthermore, the small energy budget involved in u⟷d flips is consistent with the ubiquity of the $\beta^{\pm}$-decays via weak interactions [24][41].[4]

b. The decays s→u, s→d release substantial amounts of energy (126-127 MeV). This energy is ∼64% larger than the isospin transition energy of 76.96 MeV quoted in equation (B.8) above; comparable to the differences in rest-mass between $\Sigma$ and $\Xi$ baryons (Figure 4); and also comparable to the rest-masses (Table 3) of the pions emitted in $\Xi \to \Lambda^0\,\pi$ decays (Table 5).

c. The energy release from $\delta I = -1/2$ changes is small (e.g., $EI_{1/2\to 0} = -38.65$ MeV, about 30% of $E_{\text{u}\to\text{s}}$), but this energy also becomes available to the surrounding strong fields for other tasks.

d. A curious finding is the following: We define by $E > 0$ the energy needed to support a quark flip to a higher-mass s quark (i.e., d→s or u→s, as in equation (B.7)), plus the 1-MeV anti-Coulombic contribution of u→s in $n^0 \to \Sigma^-$ (§ 3.3); and by $\delta m > 0$ the rest-energy differential between the two quarks; then, we find that the corresponding "mass deficit" is effectively the same in both cases, viz.

$$MD_{\text{u,d}\to\text{s}} \equiv (E - \delta m)_{\text{u,d}\to\text{s}} = 37\text{MeV}; \tag{B.10}$$

as it should be, since EM forces and quark rest-mass differences have been accounted for, and the isospin energy $EI_{1/2\to 0}$ is the same in both cases ($I_3 = 0$ for the s quark; Table 4).

e. Despite the similarity between cases in item (d), the decay s→u dominates entirely in nature (s→d, in which $Q = -1/3 \to -1/3$, does not occur), but for an EM-related reason: Virtual neutral vector bosons $Z^0$ do not mediate quark transitions [4][24], and $W^{\pm}$ bosons always modify the quark charge.

This prevents the weak s→d transition and makes the EM charge factor of $\vartheta_{\mathrm{e}} = 2$ (§ 2.2) all the more important for the quarks that own it (residing in u- and c-flavored hadrons).

### *Appendix B.3. Octet Ξ baryons*

The Ξ baryons contain two s quarks, in contrast to $\Lambda^0$ (one s quark), and they undergo only the decays $\Xi \to \Lambda^0 \pi$ (Table 5). We have analyzed the energy budget of the transitions $\Lambda^0 \to \Xi$ in the same way and with the same assumptions as above, and we have obtained the transition energies necessary to support the appearance of the second s quark in Ξ baryons. By doing so, we have shifted our analysis into the second highest energy level of excited states in the $J^{\mathrm{P}} = (1/2)^+$ baryon octet; these states are effectively defined by the birth of the second s quark from first-generation quarks. The same results can be obtained by considering the transitions $n^0 \to \Xi$, in which two s quarks are born together, and the isospin ( $I = 1/2$) does not change and does not play a role.

Here we summarize the energy breakdown of the various processes responsible for the appearance of the second s quark ($\Lambda^0 \to \Xi^0$ where $\mathrm{d}\to\mathrm{s}^{(2)}$, and $\Lambda^0 \to \Xi^-$ where $\mathrm{u}\to\mathrm{s}^{(2)}$). The isospin changes from $I = 0$ to $I = 1/2$ in both cases. The energy remainders $ER^{(2)}$ in the strong-field support of the $\Lambda^0 \to \Xi$ excitations are

$$\left.\begin{aligned} \Lambda^0 \to \Xi^0 \ \ (\mathrm{d}\to\mathrm{s}) \ : \ \ ER^{(2)}_{\Xi^0} &= 110.45 \\ \Lambda^0 \to \Xi^- \ \ (\mathrm{u}\to\mathrm{s}) \ : \ \ ER^{(2)}_{\Xi^-} &= 113.79 \end{aligned}\right\} \mathrm{MeV}, \tag{B.11}$$

where the anti-Coulombic contribution of 1.00 MeV has been subtracted from $ER^{(2)}_{\Xi^-}$. The corresponding system of equations for the energy components of quark transitions takes the form

$$\left.\begin{aligned} E^{(2)}_{\mathrm{d}\to\mathrm{s}} + EI_{0\to1/2} &= 110.45 \\ E^{(2)}_{\mathrm{u}\to\mathrm{s}} + EI_{0\to1/2} &= 113.79 \end{aligned}\right\} \mathrm{MeV}, \tag{B.12}$$

where $EI_{0\to1/2}$ is given by equation (B.9). The solution of this system is

$$\left.\begin{aligned} E^{(2)}_{\mathrm{d}\to\mathrm{s}} &= 71.80 \\ E^{(2)}_{\mathrm{u}\to\mathrm{s}} &= 75.14 \end{aligned}\right\} \mathrm{MeV}. \tag{B.13}$$

Subtracting these two values, we find that $E^{(2)}_{\mathrm{u}\to\mathrm{d}} = 3.34$ MeV; thus, when the second s quark appears, the cost for also flipping the remaining quark (u→d) effectively doubles (hypothetical, since $\Xi^- \to \Xi^0$ does not occur).

Combining now the quark transition energies from equations (B.7) and (B.13), and rounding off to one decimal for convenience, we determine that

$$\left.\begin{array}{rcl} E_{\mathrm{uu}\to\mathrm{ss}} &=& 202.5 \\ E_{\mathrm{ud}\to\mathrm{ss}} &=& 200.0 \\ E_{\mathrm{dd}\to\mathrm{ss}} &=& 197.5 \end{array}\right\} \mathrm{MeV}. \tag{B.14}$$

Here, 2.5 MeV differences mimic differences in u and d quark rest-masses ($m_{\mathrm{d}} - m_{\mathrm{u}} = 2.5$ MeV; Table 4); but they do not stem from quark rest-masses which were taken out of the $MD$s that gave us equation (B.11). Instead, they reflect the following property of two light quarks flipping to s quarks.

We use the binding energies in equation (B.14) to derive the "mass deficits" of two-quark s-transitions (as in equation (B.10) above for one-quark s-transitions), viz.

$$MD_{\mathrm{qq'}\to\mathrm{ss}} \equiv (E - \delta m)_{\mathrm{qq'}\to\mathrm{ss}} = 20\mathrm{MeV}, \tag{B.15}$$

where qq′ represents any of the pairs (uu, dd, ud).

## *Appendix B.4. The $\Omega^-$ baryon*

Although not a member of the baryon octet, $\Omega^-$ is of special interest as it contains three s quarks. Its decays $\Omega^- \to \Xi\pi$ and $\Omega^- \to \Lambda^0\mathrm{K}^-$ also involve a change of spin $J = 3/2 \to 1/2$, whereas parity is conserved [1][2][42][24]. At the same time, the $J = 3/2$ $\Xi^*$ baryons also decay to $J = 1/2$ $\Xi$ baryons ( $\Xi^* \to \Xi\,\pi$). Thus, we have an opportunity to study the energy requirement $E^{(3)}_{\mathrm{u,d}\to\mathrm{s}}$ for a third s quark to appear in the transition $\Xi^* \to \Omega^-$, and to determine the energy $EJ_{\delta J=-1}$ released due to spin change in the transitions $\Xi^* \to \Xi$, in which isospin $I = 1/2$ and $\delta I = 0$ (see Appendix B.5).

Using the above methodology and assumptions, we find for $\Xi^* \to \Omega^-$ that

$$\left.\begin{array}{rcl} E^{(3)}_{\mathrm{d}\to\mathrm{s}} &=& 87.37 \\ E^{(3)}_{\mathrm{u}\to\mathrm{s}} &=& 87.06 \end{array}\right\} \mathrm{MeV}, \tag{B.16}$$

a somewhat surprising result ($E^{(3)}_{\mathrm{d}\to\mathrm{s}} \gtrsim E^{(3)}_{\mathrm{u}\to\mathrm{s}}$) that may yet be valid at the high energies considered here; and, by combining equations (B.14) and (B.16), that

$$\left.\begin{array}{rcl} E_{\mathrm{uuu}\to\mathrm{sss}} &\simeq& 290 \\ E_{\mathrm{ddd}\to\mathrm{sss}} &\simeq& 285 \end{array}\right\} \mathrm{MeV}. \tag{B.17}$$

We reiterate that the transition s→d does not occur in nature [4][24], so the 285-MeV cost determined here is of some theoretical interest only.

## *Appendix B.5. $\Xi^*$ baryon decays emitting pions*

The $\Xi^*$ baryons invariably decay to $\Xi$ baryons emitting a pion ($\Xi^* \to \Xi\,\pi$; Tables 6 and 9) [1][2]. The energy released in these four reactions comes from the change in spin in the transitions $\Xi^* \to \Xi$, viz.

$$\delta J = -1\,, \tag{B.18}$$

where no spin energy is stored into the $J = 0$ pion (isospin energy is included in the rest-masses of the fragments). Then, this allows for a determination of the kinetic energy $KE_\pi$ imparted to the pion in each of these decays.

From energy conservation in the decays $\Xi^* \to \Xi\,\pi$, we find that

$$KE_\pi = 77.8^{+4.1}_{-7.3}\,\mathrm{MeV}. \tag{B.19}$$

This average value compares well to the 77-MeV of energy released in the decay $\Sigma^0 \to \Lambda^0\,\gamma$ due to the change in isospin $\delta I = -1$. Thus, this is another instance where isospin behaves quantitatively like spin (which was the basis for Heisenberg's original design of the isospin vector [43]).

The error bar in $KE_\pi$ indicates missing physics in intermediate steps (weak interactions), mostly in the decays of $\Xi^{*0}$ that resulted in the largest deviations from the mean. The decay $\Xi^{*0} \to \Xi^-\,\pi^+(+70.5\,\mathrm{MeV})$ is particularly noted because charges appear "out of nowhere" and the cost of creating charge in an initial neutral state is unknown.

Because pions are emitted also in kaon decays, we can obtain independent estimates of their shared kinetic energy. In particular, kaons exhibit a set of hadronic modes (most with significant frequencies of occurrence $\Gamma_i/\Gamma$, the so-called *branching ratios*), some of which produce three pions [1][2][24], viz.

$$\left.\begin{array}{ll} \mathrm{K}^\pm \to \pi^+\pi^-\pi^\pm, & \Gamma_{11}/\Gamma = 5.583\,\% \\ \mathrm{K}^0_{(\mathrm{L})} \to \pi^+\pi^-\pi^0, & \Gamma_7/\Gamma = 12.54\,\% \end{array}\right\}. \tag{B.20}$$

From energy conservation in these reactions, we find that the average total kinetic energy imparted to the three pions is

$$KE_{3\pi} = 77.8^{+5.7}_{-2.8}\,\mathrm{MeV}. \tag{B.21}$$

The error bar here is however shorter by about 3 MeV than that in equation (B.19). Apparently then, an energy release of about 77 MeV is common in hadron decays in which pions or photons are being emitted.

The $KE_{3\pi}$ value in equation (B.21) is the smallest amount of total kinetic energy that can be produced in nonet hadronic modes because nonet kaons do not have enough energy to decay to four pions. For comparison purposes, the $\omega$ vector meson that can decay to four pions ($\omega \to 2\pi^+\,2\pi^-$, $\Gamma_{12}/\Gamma < 0.1\,\%$) imparts a total $KE_{4\pi} = 224$ MeV ($\sim$3 times as much) to the pions.

## *Appendix C. Valence antiquarks in K and π pseudoscalar mesons*

Nonet $J^{\mathrm{P}} = 0^{-}$ kaons decay to pions with an isospin change per pion of

$$\delta I = +1/2\,, \tag{C.1}$$

and no spin-parity (CP) change across the reactions ($\delta J^{\delta \mathrm{P}} = 0^{0}$). An examination of (anti)quark flipping in $\mathrm{K} \to \pi$ transitions allows us to investigate the energy budget of antiquarks. The results are not simply a dry overview of those obtained for quarks in Appendix B. As we will see, the antiquarks have different transition energies $E_{\bar{\mathrm{q}} \to \bar{\mathrm{q}}'}$ and different energy levels, in which $\bar{\mathrm{d}}$ appears to be the actual ground state.

Using again the methodology and the assumptions of Appendix B, we find for $\pi^{0} \to \mathrm{K}^{0}$ (where $\pi^{0}$ is approximately the mixed state $(\mathrm{u}\bar{\mathrm{u}} - \mathrm{d}\bar{\mathrm{d}})/\sqrt{2}$ that the energy remainder is

$$\left.\begin{aligned} \pi^{0} \to \mathrm{K}^{0}\ (\mathrm{u}\bar{\mathrm{u}} \to \mathrm{d}\bar{\mathrm{s}})\ :\ \ ER_{\mathrm{u}\bar{\mathrm{u}}} &= 271.39\,\mathrm{MeV} \\ \pi^{0} \to \mathrm{K}^{0}\ (\mathrm{d}\bar{\mathrm{d}} \to \mathrm{d}\bar{\mathrm{s}})\ :\ \ ER_{\mathrm{d}\bar{\mathrm{d}}} &= 271.39\,\mathrm{MeV} \end{aligned}\right\}. \tag{C.2}$$

The value of $ER_{\pm}$ in charged transitions ($\pi^{\pm} \to \mathrm{K}^{\pm}$) is 6.02 MeV smaller, and it will not be used in the calculations that follow. The origin of the difference is purely electromagnetic; this value is the sum of the 4.59 MeV difference in pions and the 1.43 MeV difference in kaons (*MD* values are listed in Table 3).

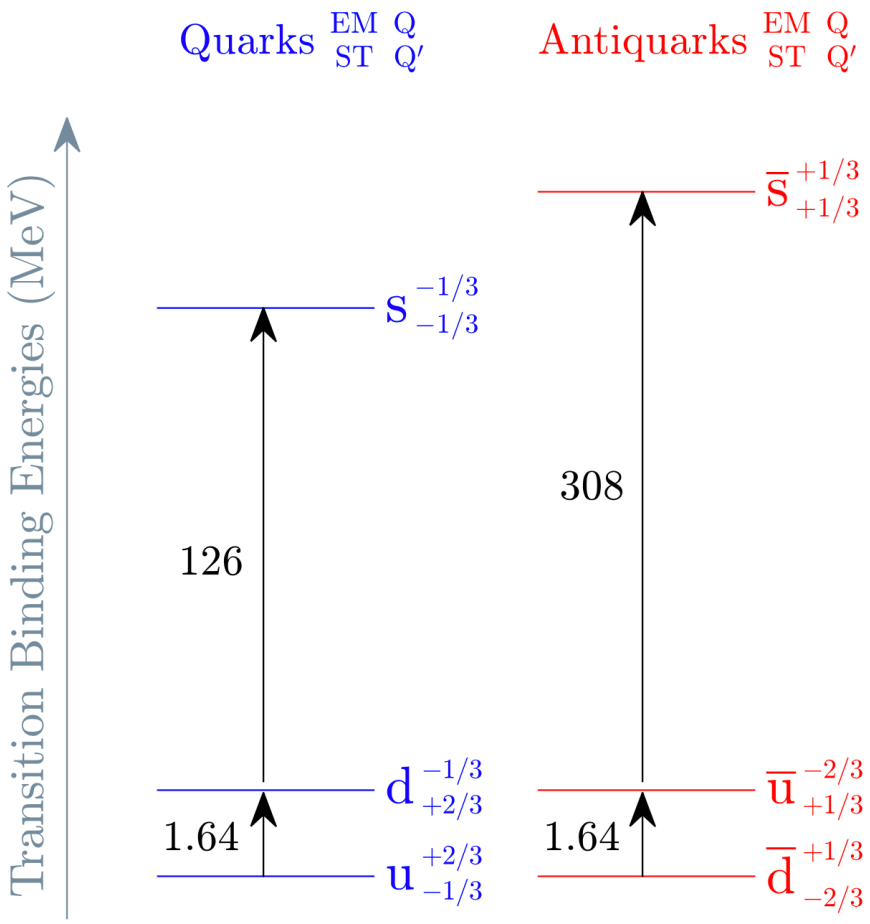


**Figure C1.** Quark and antiquark transition energies for the three lower-energy states in each group. The diagram is drawn on a logarithmic scale. Binding energy jumps are quoted to three significant digits. The binding energy of $\bar{u} \to \bar{s}$ is 2.4 times larger than that of the u→s transition, pointing to the origin of CP violation.

Using the (anti)quark transitions in equation (C.2), we derive the following system of equations:

$$\left.\begin{array}{rcl} E_{u\to d} + E_{\bar{u}\to\bar{s}} + EI_{1\to 1/2} & = & 271.39 \\ E_{\bar{d}\to\bar{s}} + EI_{1\to 1/2} & = & 271.39 \end{array}\right\} \text{MeV}, \tag{C.2}$$

where $E_{u\to d} = 1.64$ MeV and $EI_{1\to 1/2} = -38.31$ MeV (Appendix B). The solution of system (C.3) is

$$\left.\begin{array}{rcl} E_{\bar{u}\to\bar{s}} & = & 308.06 \\ E_{\bar{d}\to\bar{s}} & = & 309.70 \end{array}\right\} \text{MeV}, \tag{C.4}$$

from which we obtain an astonishing result:

$$E_{\bar{u}\to\bar{d}} = -1.64\text{MeV}; \tag{C.5}$$


doi.org/10.32388/ZM7QNO

that is, the antiquark transition $\bar{\mathrm{u}} \rightarrow \bar{\mathrm{d}}$ releases energy back to the strong field. This implies that $\bar{\mathrm{d}}$ is the actual antiquark ground state, and it lies below $\bar{\mathrm{u}}$ by the same amount of binding energy (1.64 MeV) as the u-quark ground state lies below the d quark.

The same results precisely have also been obtained by two alternative calculations: (a) By considering the equations for the alternative (anti)quark paths ($\mathrm{u} \rightarrow \bar{\mathrm{s}}$, $\bar{\mathrm{u}} \rightarrow \mathrm{d}$) and ($\mathrm{d} \rightarrow \bar{\mathrm{s}}$, $\bar{\mathrm{d}} \rightarrow \mathrm{d}$); and (b) by considering the path $\left(\mathrm{u}\bar{\mathrm{u}} + \mathrm{d}\bar{\mathrm{d}}\right)/2 \rightarrow \mathrm{K}^0$. These results imply that the systems of equations that we solve on these paths are self-consistent; at the same time, the equations imply that there is no preferred path in (anti)quark flips during the $\pi^0 \rightarrow \mathrm{K}^0$ transitions, since all paths are energetically equivalent.

The energy budgets for quark and antiquark transitions are illustrated in Figure C1 assuming that the two ground states lie at the same energy level. It appears that strong-field support of the $\bar{\mathrm{s}}$ antiquark in a bound state is about 2.4 times more expensive than that of the s quark; and this is grounds for the emergence of CP violation (see also item (4b) in § 6.2 of the main text).

## Acknowledgments

NASA support over the years is gratefully acknowl- edged. DMC also acknowledges support from NSF-AAG grant No. AST-2109004.

## Data availability statement

The data analyzed in this work are publicly available from the Particle Data Group [1][2] and CODATA [3]. Summarizing tables can be obtained from Wikipedia (https://en.wikipedia.org/wiki/List_of_baryons, https://en.wikipedia.org/wiki/List of mesons).

## Footnotes

[1] Calculations of the total EM potential energy ($PE$) of the quarks in each of the particles depicted in Figures 7-9 below provide a crucial hint: $PE < 0$ and binding for both $\pi^0$ and $\pi^0$; whereas $PE \geq 0$ for $\pi^{\pm}$ and $p^{\pm}$, respectively.

[2] The neutral particle not having the lowest $MD$ in its group is a singular property of only 5 excited states. In particular, it occurs in $\Sigma^{0,+}$ ($\delta_{MD} = 0.76$ MeV) and $\Xi^{0,+}$ ($\delta_{MD} = 0.40$ MeV) baryons (Table 1); and in $\mathrm{K}^{0,+}$ ($\delta_{MD} = 1.42$ MeV), $\rho^{0,+}$ ($\delta_{MD} = 0.15$ MeV), and $\mathrm{K}^{*0,+}$ ($\delta_{MD} = 1.64$ MeV) mesons (Table 3). The same effect may also be real in $\Delta^{0,-}$ baryons (Table 2).

[3] The Casimir charge $C_F = 4/3$ commonly appears in SU(3) in strong interactions. For instance, it helps define the short-range term of the potential energy of the quarkonia $\bar{\mathrm{c}}$ and $\bar{\mathrm{b}}$[44][28].

[4] There is no energy charge for $I_3 = \pm 1/2 \rightarrow \mp 1/2$ changes in u$\longleftrightarrow$d flips, as we already know from the $p^+$-$n^0$ results of § 3.1.

## References


1. a, b, c, d, e, f, g, h, i Zyla, P. A., et al. (2020). Review of particle physics. Progress in Theoretical and Experimental Physics, 2020(8), 083C01.
2. a, b, c, d, e, f, g, h, i, j Workman, R. L., et al. (2022). Review of particle physics. Progress in Theoretical and Experimental Physics, 2022(8), 083C01.
3. a, b, c Tiesinga, E., et al. (2021). CODATA recommended values of the fundamental physical constants: 2018. Review of Modern Physics, 93, 025010.
4. a, b, c, d, e, f Peskin, M. E., & Schroeder, D. V. (1995). An introduction to quantum field theory. CRC Press.
5. ^ Durr, S., et al. (2008). Ab initio determination of light hadron masses. Science, 322, 1224.
6. ^ Yang, Y. B., et al. (2018). Proton mass decomposition from the QCD energy momentum tensor. Physical Review Letters, 121, 212001.
7. ^ Metz, A., et al. (2022). Understanding the proton mass in QCD. SciPost Physics Proceedings, 8, 105.
8. a, b, c Pohl, R., et al. (2010). The size of the proton. Nature, 466, 213.
9. a, b, c Antognini, A., et al. (2013). Proton Structure from the Measurement of 2S-2P Transition Frequencies of Muonic Hydrogen. Science, 339, 417.
10. a, b, c Bezginov, N., et al. (2019). A measurement of the atomic hydrogen Lamb shift and the proton charge radius. Science, 365, 1007.
11. a, b, c Xiong, W., et al. (2019). A small proton charge radius from an electron–proton scattering experiment. Nature, 575, 147.
12. a, b, c Karr, J. P., Marchand, D., & Voutier, E. (2020). The proton size. Nature Reviews Physics, 2, 601.
13. a, b, c, d Ericson, T., & Weise, W. (1988). Pions and nuclei. Oxford University Press.
14. ^ Duran, B., et al. (2023). Determining the gluonic gravitational form factors of the proton. Nature, 615, 813.
15. ^ Bars, I., & Hanson, A. J. (1976). Quarks at the ends of the string. Physical Review D, 13, 1744.
16. ^ Kalashnikova, Y. S., & Nefediev, A. V. (1997). 1+1 string with quarks at the ends revisited. Physics Letters B, 399, 274.

17. ^Nefediev, A. V. (2002). Light-light and heavy-light mesons in the model of QCD string with quarks at the e nds. AIP Conference Proceedings, 619, 595.

18. ^Pasechnik, R., & Šumbera, M. (2017). Phenomenological review on quark–gluon plasma: Concepts vs. obser vations. MDPI/Universe, 3, 7.

19. ^Fritzsch, H. (2018). Quarks. In Murray Gell-Mann and the physics of quarks. Birkhauser.

20. ^Bulava, J., et al. (2019). String breaking by light and strange quarks. Physics Letters B, 793, 493.

21. ^Nakano, T., & Nishijima, K. (1953). Charge independence for V-particles. Progress in Theoretical Physics, 10, 581.

22. ^Nishijima, K. (1955). Charge independence theory of V particles. Progress in Theoretical Physics, 13, 285.

23. ^Gell-Mann, M. (1956). The interpretation of the new particles as displaced charge multiplets. Nuovo Cimen to, 4(Suppl 2), 848.

24. a, b, c, d, e, f, g, h, i, jRohlf, J. W. (1994). Modern physics. John Wiley.

25. a, bPovh, B., et al. (2004). Particles and nuclei (4th ed.). Springer-Verlag.

26. ^Christman, J. R. (2001). Isospin: Conserved in strong interactions. Retrieved from https://www.physnet.org/ modules/pdf_modules/m278.pdf

27. ^Miller, A. I. (2009). 137: Jung, Pauli, and the Pursuit of a Scientific Obsession. WWNorton.

28. a, b, cBali, G. S. (2001). QCD forces and heavy quark bound states. Physics Reports, 343, 1.

29. ^Dimopoulos, S., & Susskind, L. (1978). Baryon number of the universe. Physical Review D, 18, 4500.

30. ^Shaposhnikov, M. E., & Farrar, G. R. (1993). Baryon asymmetry of the universe in the Minimal Standard Mo del. Physical Review Letters, 70, 2833.

31. ^Riotto, A., & Trodden, M. (1999). Recent progress in baryogenesis. Annual Review of Nuclear and Particle S cience, 49, 46.

32. ^Canetti, L., et al. (2012). Matter and antimatter in the universe. New Journal of Physics, 14, 095012.

33. ^The LHCb Collaboration. (2017). Measurement of matter–antimatter differences in beauty baryon decays. Nature Physics, 13, 391.

34. ^The LHCb Collaboration. (2019). Observation of CP violation in charm decays. Physical Review Letters, 12 2, 211803.

35. ^Davies, C. T. H., et al. (2004). High-precision lattice QCD confronts experiment. Physical Review Letters, 92, 022001.

36. ^DeGrand, T., & DeTar, C. (2006). Lattice methods for quantum chromodynamics. World Scientific.

37. ^ *Gattringer, C., & Lang, C. B. (2010). Quantum chromodynamics on the lattice. Springer.*

38. ^ *Bazanov, A. (2010). Nonperturbative QCD simulations with 2+1 flavors of improved staggered quarks. Revi ew of Modern Physics, 82, 1349.*

39. ^ *Petreczky, P. (2012). Lattice QCD at non-zero temperature. Journal of Physics G: Nuclear and Particle Physi cs, 39, 093002.*

40. ^ *Rafelski, J. (2015). Melting hadrons, boiling quarks. European Physical Journal A, 51, 114.*

41. ^ *Kónya, J., & Nagy, N. M. (2018). Nuclear and radiochemistry (2nd ed.). Elsevier.*

42. ^ *Barnes, V. E., et al. (1964). Observation of a hyperon with strangeness minus three. Physical Review Letters, 12, 204.*

43. ^ *Heisenberg, W. (1932). Über den Bau der Atomkerne. I. Zeitschrift für Physik, 77, 1.*

44. ^ *Eichten, E., et al. (1978). Charmonium: The model. Physical Review D, 17, 3090.*

## Declarations

**Funding:** No specific funding was received for this work.

**Potential competing interests:** No potential competing interests to declare.